

Grounded partitions of type $A_1^{(1)}$ at levels 1 and 2: bijections, affine crystal graphs, and partition identities

Benedek Dombos* Jihyeug Jang†

December 19, 2025

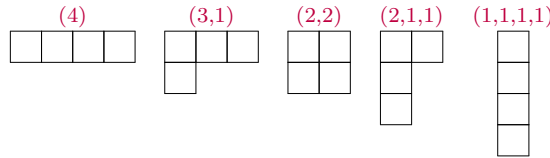
Abstract

Grounded partitions, introduced by Dousse and Konan, are coloured partitions satisfying difference conditions given by a matrix with nonnegative integer entries. For the matrices studied in this paper, the generating functions are known to be infinite products, corresponding to the principal specialisation of characters of highest weight modules of type $A_1^{(1)}$. We give the first bijective proof that the generating functions of grounded partitions at level 2 are infinite products. We then give a new combinatorial model for affine crystal graphs of type $A_1^{(1)}$ at level 2, where the vertices are grounded partitions and the arrows are given by explicit bracketing rules. The grounded partition model for affine crystal graphs of highest weights Λ_0 , Λ_1 and $\Lambda_0 + \Lambda_1$ gives rise to new q -series identities obtained by decomposing the affine crystal graphs into the crystal graphs of finite type A_1 via the restricted representation.

1 Introduction

A *partition* of a nonnegative integer n is a non-increasing sequence $\lambda = (\lambda_1, \lambda_2, \dots, \lambda_k)$ of positive integers such that $n = \lambda_1 + \lambda_2 + \dots + \lambda_k$. The integers λ_i are called the *parts* of the partition λ . The number of parts k is called the *length* of λ , and is denoted by $\ell(\lambda)$. The sum of the terms is called the *size* of λ , denoted $|\lambda|$. The empty sequence corresponds to the unique partition of size 0, called the *empty partition*.

For example, there are five partitions of size 4: (4) , $(3, 1)$, $(2, 2)$, $(2, 1, 1)$, and $(1, 1, 1, 1)$. We identify partitions with their *Young diagrams*:



In the theory of integer partitions, it is convenient to abbreviate some finite and infinite products by *q-Pochhammer symbols*. For formal variables a and q , define

$$(a; q)_k := (1 - a)(1 - aq)(1 - aq^2) \cdots (1 - aq^{k-1}), \quad \text{for } k \geq 1,$$

$$(a; q)_0 := 1, \quad (a; q)_\infty := \prod_{k=0}^{\infty} (1 - aq^k).$$

*benedek.dombos@unige.ch, University of Geneva
 †jihyeug.jang@unige.ch, University of Geneva

We also use the shorthand notation:

$$(a_1, \dots, a_\ell; q^n)_\infty := (a_1; q^n)_\infty \cdots (a_\ell; q^n)_\infty.$$

Example 1.1. (i) The size generating function of partitions into distinct parts is given by the following infinite product:

$$\sum_{\lambda \in \mathcal{D}} q^{|\lambda|} = \prod_{i=1}^{\infty} (1 + q^i) = (-q; q)_\infty,$$

where \mathcal{D} denotes the set of distinct-part partitions. In each factor $(1 + q^i)$ we have two choices: we either have i as a part or we do not

Any distinct-part partition with n parts can be decomposed uniquely as a sum of a staircase shape $(n, n-1, \dots, 2, 1)$ with n parts and another partition with at most n parts. This shows the following identity (see the book by Stanley [26, Proposition 1.8.6 (c)]):

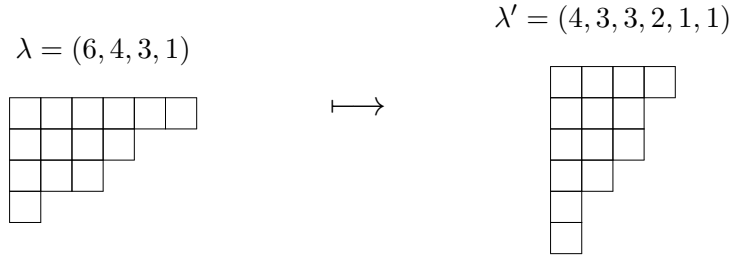
$$(-q; q)_\infty = \sum_{n=0}^{\infty} \frac{q^{\binom{n+1}{2}}}{(q; q)_n}. \tag{1.1}$$

The left-hand side of this identity can also be written as the infinite product:

$$(-q; q)_\infty = \frac{1}{(q; q^2)_\infty},$$

which is the generating function of partitions into odd parts.

(ii) Partitions of n with distinct parts are in bijection with partitions of n where the difference between consecutive parts is at most 1 and for nonempty partitions, 1 appears as a part. This bijection is given by *conjugation*, i.e. by reflecting the Young diagram of a partition λ with distinct parts across the main diagonal. This operation is illustrated as



The image of λ is called the *conjugate* of λ , denoted λ' .

Partition identities of the form: the number of partitions of n with certain congruence conditions on the parts equals the number of partitions of n with certain difference conditions on the parts, are called identities of *Rogers–Ramanujan type*, named after the following theorem.

Theorem 1.2 (Rogers–Ramanujan identities, in terms of q -series, [23]).

$$\sum_{n=0}^{\infty} \frac{q^{n^2}}{(q; q)_n} = \frac{1}{(q; q^5)_\infty (q^4; q^5)_\infty}, \quad \sum_{n=0}^{\infty} \frac{q^{n^2+n}}{(q; q)_n} = \frac{1}{(q^2; q^5)_\infty (q^3; q^5)_\infty}. \tag{1.2}$$

Each of these q -series identities corresponds to a partition identity. Here, we only state the first identity (see [22] and [24] for further details). The number of partitions of n such that the difference between consecutive parts is at least 2 is equal to the number of partitions of n into parts congruent to 1 or 4 (mod 5). Finding an explicit and simple size-preserving bijection between these two sets is one of the most notoriously elusive open problems in enumerative combinatorics.

Remark 1.3. That the left-hand side of the first Rogers–Ramanujan identity (1.2) is the generating function for partitions whose consecutive parts differ by at least two follows from a staircase argument similar to Example 1.1 (i). In this case, we decompose the partition into an odd staircase $(2n - 1, 2n - 3, \dots, 3, 1)$ of length n and an arbitrary partition of length at most n . The size of the odd staircase is n^2 .

Lepowsky and Wilson [20, 21] gave a representation-theoretic proof of the Rogers–Ramanujan identities, building on earlier work of Lepowsky and Milne [19]. The product side can be obtained directly from the principal specialisation of the Weyl–Kac character formula (see the book by Kac [15, Theorem 10.4]), for characters of highest weight modules of type $A_1^{(1)}$ at level 3. The representation-theoretic interpretation of the sum side is more intricate. In these papers, Lepowsky and Wilson developed and applied the theory of vertex operators to derive it. An alternative approach is to study partitions with difference conditions via the theory of affine and perfect crystals; see Dousse–Konan [8, 9]. A representation-theoretic introduction to this topic is given in the book by Hong and Kang [14].

1.1 Grounded partitions

Grounded partitions are combinatorial objects introduced by Dousse and Konan in [8] and [9], motivated by the theory of perfect crystals (introduced by Kang, Kashiwara, Misra, Miwa, Nakashima, and Nakayashiki [16]). In this paper, we consider a specific family of grounded partitions $\mathcal{P}_{n,i}$ for a nonnegative integer n and a colour c_i , defined below. Here, we define only a simplified version of grounded partitions with exact difference conditions, which will be sufficient for our purposes.

Definition 1.4. Let n be a nonnegative integer, and let $C_n = \{c_0, c_1, \dots, c_n\}$ be a set of *colours*. Define M_n to be the square matrix of size $n + 1$ whose (i, j) -entry is $|n + 2 - i - j|$, that is,

$$M_n = \begin{bmatrix} n & n-1 & n-2 & & 2 & 1 & 0 \\ n-1 & n-2 & n-3 & \dots & 1 & 0 & 1 \\ n-2 & n-3 & n-4 & & 0 & 1 & 2 \\ & \vdots & & \ddots & & \vdots & \\ 2 & 1 & 0 & & n-4 & n-3 & n-2 \\ 1 & 0 & 1 & \dots & n-3 & n-2 & n-1 \\ 0 & 1 & 2 & & n-2 & n-1 & n \end{bmatrix}.$$

Fix a colour $c_i \in C_n$. A *grounded partition* $\pi = (\pi_0, \pi_1, \dots, \pi_s)$ corresponding to the matrix M_n with *ground* 0_{c_i} is a sequence of positive integers, each indexed by a colour in C_n , except for the initial part $\pi_0 = 0_{c_i}$, satisfying the following exact difference condition: for $j \geq 0$, let π_j and π_{j+1} be two consecutive parts of sizes $|\pi_j|$ and $|\pi_{j+1}|$ with colours c_{i_j} and $c_{i_{j+1}}$, respectively. Then

$$|\pi_{j+1}| - |\pi_j| = (i_{j+1}, i_j)\text{-entry of } M_n.$$

We denote by $\mathcal{P}_{n,i}$ the set of grounded partitions corresponding to the matrix M_n with ground 0_{c_i} . For a grounded partition π , the number of nonzero parts is called the *length* of π , denoted by $\ell(\pi)$. The *size* of π is defined as the size of the underlying partition obtained by forgetting the colours, denoted $|\pi|$. For convenience, we omit the ground π_0 , and write $\pi = (\pi_0, \pi_1, \pi_2, \dots, \pi_s)$ simply as $\pi_1 \pi_2 \cdots \pi_s$.

Partitions are typically written in weakly decreasing order. For grounded partitions, however, we list parts in weakly increasing order, as the colour of the final 0 part is significant. This is equivalent to reversing the usual notation.

Recently, Dousse, Hardiman, and Konan [7] gave a product formula for the generating function for grounded partitions in $\mathcal{P}_{n,i}$.

Theorem 1.5 ([7, Theorem 1.6]). Let n and i be integers with $0 \leq i \leq n$. Then, the generating function for grounded partitions in $\mathcal{P}_{n,i}$ is given by

$$\sum_{\lambda \in \mathcal{P}_{n,i}} q^{|\pi|} = \frac{(q^{i+1}, q^{n-i+1}, q^{n+2}; q^{n+2})_{\infty}}{(q; q^2)_{\infty} (q; q)_{\infty}}.$$

They used the character formula for perfect crystals corresponding to the standard modules of the affine Lie algebra $A_1^{(1)}$ at level n , of highest weight $i\Lambda_0 + (n-i)\Lambda_1$. Using the associated energy matrices, they showed that this character formula coincides with the generating function for grounded partitions $\mathcal{P}_{n,i}$, and obtained the right-hand side via the principal specialization of the Weyl–Kac character formula.

Remark 1.6. Our matrices M_n differ slightly from those appearing in [7], which can be obtained by reflecting M_n across the vertical line in the middle. Both of these arise from considering the effect of principal specialisation on the energy matrix, a central object in the theory of perfect crystals (see [14, Chapter 10], for further details). There is a simple bijection between grounded partitions arising from the matrix M_2 and from the reflected matrix. Considering the matrices M_2 , there are explicit combinatorial rules for the arrows in the affine crystal graph, which we prove in Section 3. It would be interesting to find similarly explicit combinatorial rules for the reflected matrix.

We begin by presenting several examples. For clarity of notation, we denote the colours by $(c_0, c_1, c_2, c_3) = (a, b, c, d)$ throughout this paper. We consider only the following three matrices for M_n :

$$M_1 = \begin{array}{c|cc} & a & b \\ \hline a & 1 & 0 \\ b & 0 & 1 \end{array} \quad M_2 = \begin{array}{c|ccc} & a & b & c \\ \hline a & 2 & 1 & 0 \\ b & 1 & 0 & 1 \\ c & 0 & 1 & 2 \end{array} \quad M_3 = \begin{array}{c|cccc} & a & b & c & d \\ \hline a & 3 & 2 & 1 & 0 \\ b & 2 & 1 & 0 & 1 \\ c & 1 & 0 & 1 & 2 \\ d & 0 & 1 & 2 & 3 \end{array} \quad (1.3)$$

In the examples below, we usually omit the ground in the notation at the beginning of each grounded partition. The ground is always clear from context, as we specify the set of grounded partitions in advance. We write $0_b \in \mathcal{P}_{2,b}$ for the empty partition, using the subscript b to indicate the ground. This is the unique grounded partition of size zero.

Example 1.7. (i) We list the elements of $\mathcal{P}_{1,b}$ of size 7. Here the ground is 0_b .

$$1_b 1_a 1_b 1_a 1_b 1_a 1_b, \quad 1_b 1_a 1_b 1_a 1_b 2_b, \quad 1_b 1_a 1_b 2_b 2_a, \quad 1_b 2_b 2_a 2_b, \quad 1_b 1_a 2_a 3_a$$

In this case, the colours are completely determined by the size of the parts, and by forgetting the colours, we recover the conjugate distinct-part partitions of Example 1.1. Their size generating function

$$\sum_{\pi \in \mathcal{P}_{1,b}} q^{|\pi|} = 1 + q + q^2 + 2q^3 + 2q^4 + 3q^5 + 4q^6 + 5q^7 + 6q^8 + \dots, \quad (1.4)$$

equals the infinite product $(-q; q)_{\infty}$, as shown bijectively in Example 1.1.

(ii) There is a simple size-preserving bijection between $\mathcal{P}_{1,b}$ and $\mathcal{P}_{1,a}$, by swapping the colours a and b . Thus, the size generating function of $\mathcal{P}_{1,a}$ is the same infinite product.

(iii) We list the elements of $\mathcal{P}_{2,b}$ for sizes ranging from 0 to 6, as they will be used explicitly in Subsection 2.1:

- Size 0: 0_b
 Size 1: $1_a, 1_c$
 Size 2: $1_a 1_c, 1_c 1_a$
 Size 3: $1_a 1_c 1_a, 1_c 1_a 1_c, 1_a 2_b, 1_c 2_b$
 Size 4: $1_a 1_c 1_a 1_c, 1_c 1_a 1_c 1_a, 1_a 1_c 2_b, 1_c 1_a 2_b, 1_a 3_a, 1_c 3_c$
 Size 5: $1_a 1_c 1_a 1_c 1_a, 1_c 1_a 1_c 1_a 1_c, 1_a 1_c 1_a 2_b, 1_c 1_a 1_c 2_b, 1_a 2_b 2_b, 1_c 2_b 2_b, 1_a 1_c 3_c, 1_c 1_a 3_a$
 Size 6: $1_a 1_c 1_a 1_c 1_a 1_c, 1_c 1_a 1_c 1_a 1_c 1_a, 1_a 1_c 1_a 1_c 2_b, 1_c 1_a 1_c 1_a 2_b, 1_a 1_c 2_b 2_b, 1_c 1_a 2_b 2_b, 1_a 1_c 1_a 3_a, 1_c 1_a 1_c 3_c, 1_a 2_b 3_a, 1_a 2_b 3_c, 1_c 2_b 3_a, 1_c 2_b 3_c$

Theorem 1.5 states that the size generating function has the following infinite product form:

$$\sum_{\pi \in \mathcal{P}_{2,b}} q^{|\pi|} = \frac{(-q; q^2)_\infty}{(q; q^2)_\infty} = 1 + 2q + 3q^2 + 5q^3 + 8q^4 + 12q^5 + 18q^6 + \dots \quad (1.5)$$

(iv) We list the elements of $\mathcal{P}_{2,a}$ for sizes ranging from 0 to 6, as they will be used explicitly in Subsection 2.2:

- Size 0: 0_a
 Size 1: 1_b
 Size 2: $2_a, 1_b 1_b$
 Size 3: $1_b 2_a, 1_b 2_c, 1_b 1_b 1_b$
 Size 4: $1_b 1_b 2_a, 2_a 2_c, 1_b 1_b 2_c, 1_b 1_b 1_b 1_b$
 Size 5: $1_b 2_a 2_c, 2_a 3_b, 1_b 2_c 2_a, 1_b 1_b 1_b 2_a, 1_b 1_b 1_b 2_c, 1_b 1_b 1_b 1_b 1_b$
 Size 6: $2_a 4_a, 2_a 2_c 2_a, 1_b 1_b 2_a 2_c, 1_b 2_a 3_b, 1_b 2_c 3_b, 1_b 1_b 2_c 2_a, 1_b 1_b 1_b 1_b 2_a, 1_b 1_b 1_b 1_b 2_c, 1_b 1_b 1_b 1_b 1_b 1_b$

By Theorem 1.5, their generating function has the following infinite product form:

$$\sum_{\pi \in \mathcal{P}_{2,a}} q^{|\pi|} = \frac{(-q^2; q^2)_\infty}{(q; q^2)_\infty} = 1 + q + 2q^2 + 3q^3 + 4q^4 + 6q^5 + 9q^6 + \dots \quad (1.6)$$

(v) By Theorem 1.5 again, the generating functions for $\mathcal{P}_{3,b}$ and $\mathcal{P}_{3,a}$ are given by

$$\sum_{\pi \in \mathcal{P}_{3,b}} q^{|\pi|} = \frac{1}{(q; q^2)_\infty} \frac{1}{(q; q^5)_\infty (q^4; q^5)_\infty} = 1 + 2q + 3q^2 + 5q^3 + 8q^4 + 12q^5 + 18q^6 + \dots, \quad (1.7)$$

$$\sum_{\pi \in \mathcal{P}_{3,a}} q^{|\pi|} = \frac{1}{(q; q^2)_\infty} \frac{1}{(q^2; q^5)_\infty (q^3; q^5)_\infty} = 1 + q + 2q^2 + 4q^3 + 5q^4 + 8q^5 + 12q^6 + \dots \quad (1.8)$$

These are the product sides of the Rogers–Ramanujan identities in Theorem 1.2, together with a fudge factor $1/(q; q^2)_\infty$. The elements of $\mathcal{P}_{3,b}$ of size 6 are

$$\begin{aligned} & 1_b 1_c 1_b 1_c 1_b 1_c, 1_d 1_a 1_d 1_a 1_d 1_a, 1_b 1_c 1_b 1_c 2_a, 1_b 1_c 1_b 1_c 2_c, 1_d 1_a 1_d 1_a 2_c, \\ & 1_b 1_c 2_a 2_d, 1_b 1_c 2_c 2_b, 1_d 1_a 2_c 2_b, 1_b 1_c 1_b 3_a, 1_d 1_a 1_d 3_c, 1_b 2_b 3_b, 1_b 2_b 3_d, \\ & 1_b 2_d 3_b, 1_d 2_b 3_b, 1_d 2_b 3_d, 2_a 2_d 2_a, 1_d 1_a 4_a, 2_a 4_b, \end{aligned}$$

and the elements of $\mathcal{P}_{3,a}$ of size 6 are

$$\begin{aligned} & 1_c 1_b 1_c 1_b 1_c 1_b, 1_c 1_b 1_c 1_b 2_b, 1_c 1_b 1_c 3_d, 1_c 1_b 2_b 2_c, 1_c 1_b 2_d 2_b, 1_c 1_b 1_c 3_d, \\ & 1_c 2_a 3_c, 1_c 2_c 3_a, 1_c 2_c 3_c, 2_b 2_c 2_b, 2_b 4_a, 3_a 3_d. \end{aligned}$$

Remark 1.8. The equality of the generating functions for $\mathcal{P}_{n,i}$ and $\mathcal{P}_{n,n-i}$ is immediately obtained from Theorem 1.5, but it also has a straightforward combinatorial proof. Since the matrix M_n is symmetric, swapping colours c_j and c_{n-j} for all j yields a size-preserving bijection between $\mathcal{P}_{n,i}$ and $\mathcal{P}_{n,n-i}$. Hence the size generating function for $\mathcal{P}_{n,i}$ is equal to that for $\mathcal{P}_{n,n-i}$. Therefore, it suffices to consider only the cases $\mathcal{P}_{1,b}$, $\mathcal{P}_{2,a}$, and $\mathcal{P}_{2,b}$ for $n = 1$ and 2 .

In Section 2, we provide bijective proofs for the identities (1.5) and (1.6), which represent the generating functions for grounded partitions at level 2. In particular, we introduce two bijections for $\mathcal{P}_{2,b}$ and $\mathcal{P}_{2,a}$, respectively. An *overpartition*, introduced by Corteel and Lovejoy [6], is a partition (nonincreasing sequence of positive integers) where the first occurrence of each number may be overlined. The first bijection, described in Subsection 2.1, goes between grounded partitions in $\mathcal{P}_{2,b}$ and overpartitions into odd parts.

Theorem 1.9. Let $\mathcal{P}_b(n, k)$ denote the set of grounded partitions in $\mathcal{P}_{2,b}$ of size n with k odd parts, and let $\overline{\mathcal{PO}}(n, k)$ denote the set of overpartitions into odd parts of size n and length k . Then, for all integers $n \geq k \geq 0$, there is a bijection between $\mathcal{P}_b(n, k)$ and $\overline{\mathcal{PO}}(n, k)$. In particular, we have

$$|\mathcal{P}_b(n, k)| = |\overline{\mathcal{PO}}(n, k)|.$$

The second bijection, described in Subsection 2.2, is obtained by modifying the first bijection.

Theorem 1.10. Let $\mathcal{P}_a(n, k)$ denote the set of grounded partitions in $\mathcal{P}_{2,a}$ of size n with k odd parts, and let $\mathcal{E}(n, k)$ denote the set of partitions of size n with k odd parts such that all even parts are distinct. Then, for all integers $n \geq k \geq 0$, there is a bijection between $\mathcal{P}_a(n, k)$ and $\mathcal{E}(n, k)$. In particular, we have

$$|\mathcal{P}_a(n, k)| = |\mathcal{E}(n, k)|.$$

We hope that the ideas developed here can be extended to give a combinatorial proof of the Rogers–Ramanujan identities (1.7) and (1.8), up to the factor $1/(q; q^2)_\infty$. Using these bijections, we obtain bijective proofs for the following refinements of (1.5) and (1.6).

Theorem 1.11. We have

$$\sum_{n \geq 0} \frac{t^n q^{n^2} (-1; q^2)_n}{(tq; q^2)_n (q^2; q^2)_n} = \frac{(-tq; q^2)_\infty}{(tq; q^2)_\infty}.$$

Theorem 1.12. We have

$$\sum_{n \geq 0} \frac{q^{n(n+1)} (-tq; q^2)_n}{(q^2; q^2)_n (tq; q^2)_{n+1}} = \frac{(-q^2; q^2)_\infty}{(tq; q^2)_\infty}.$$

We also give an alternative proof for these two identities using hypergeometric series.

Some combinatorial aspects of grounded partitions, where the matrix entries specify minimal, rather than exact, differences between consecutive parts, have been studied in [7, Section 4]. However, no bijective proof is known for the fact that the size generating function of grounded partitions with exact difference conditions is an infinite product after principal specialisation. We believe this direction is worth exploring—not only for the sake of uncovering interesting bijections (Theorems 1.9 and 1.10), but also because grounded partitions with exact difference conditions (unlike those with minimal difference conditions) admit an affine crystal structure, which will be described in detail in Section 3.

1.2 Affine crystal structures of type $A_1^{(1)}$ at levels 1 and 2

Affine crystals arise in the representation theory of affine Lie algebras. In this work, we use only combinatorial models for affine crystal graphs of type $A_1^{(1)}$ at levels 1 and 2, which we interpret as ranked posets with arrows coloured blue or green. The rank generating functions of these posets turn out to be the infinite products obtained via the principal specialisation of the corresponding characters. At level 1, there are two highest weight modules of type $A_1^{(1)}$ and highest weights Λ_0 and Λ_1 . The principal specialisation of their characters yields the same infinite product $(-q; q)_\infty$. At level two, the highest weight module of type $A_1^{(1)}$ and highest weight $\Lambda_0 + \Lambda_1$ has the principal specialisation:

$$\frac{(-q; q^2)_\infty}{(q; q^2)_\infty},$$

while the principal specialisation of the characters of type $A_1^{(1)}$ and highest weights $2\Lambda_0$ and $2\Lambda_1$ are both equal to the infinite product:

$$\frac{(-q^2; q^2)_\infty}{(q; q^2)_\infty}.$$

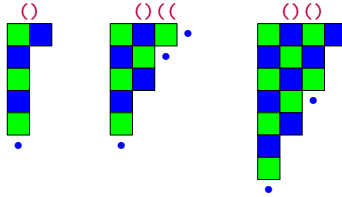
We describe a combinatorial model for the affine crystal graph of type $A_1^{(1)}$ and highest weight Λ_0 , known as the Young wall model of type $A_1^{(1)}$ on the ground-state wall Y_{Λ_0} , defined in [14, Section 11] and slightly reformulated here. The only difference from the usual model is the reading order: in the Young wall model, the reading order goes from top to bottom, whereas we read from bottom to top in order to obtain conjugate distinct-part partitions.

Definition 1.13. Given a partition λ , we consider the blue–green checkerboard pattern on λ , with a green cell in the top-left corner. A *removable blue corner* is a blue cell inside λ such that removing it still gives a partition. An *addable blue corner* is a blue cell outside λ such that adding it gives a partition. *Removable green corners* and *addable green corners* are defined in the same way.

Definition 1.14. The directed graph $\mathcal{B}_{1,b}^{\mathcal{P}}$, whose vertices are partitions and whose edges are coloured blue and green, is defined recursively starting from the empty partition. For each vertex λ , the outgoing edges are determined by the following bracketing rules:

- (i) **Blue arrow.** Assign a left bracket “(” to each addable blue corner of λ , and a right bracket “)” to each removable blue corner. Read brackets from bottom to top. If there exists an unmatched addable blue corner, add a cell at the corner corresponding to the rightmost unmatched bracket. A blue arrow is drawn from λ to the resulting partition.
- (ii) **Green arrow.** Defined in the same way, with addable and removable green corners in place of blue ones.

Example 1.15. We show a few examples of the bracketing rules from Definition 1.14. The first and third partitions have no unmatched addable blue corners, whereas the second has two:



One can verify that the vertex set of the graph $\mathcal{B}_{1,b}^{\mathcal{P}}$ is given by the conjugates of distinct-part partitions. Since the set $\mathcal{P}_{1,b}$ is naturally identified with the set of conjugate distinct-part partitions (see Example 1.7 (i)), we may regard this graph as the affine crystal graph structure on $\mathcal{P}_{1,b}$, described in terms of the bracketing rules. The affine crystal graph on the vertex set $\mathcal{P}_{1,b}$ is illustrated in Figure 1.

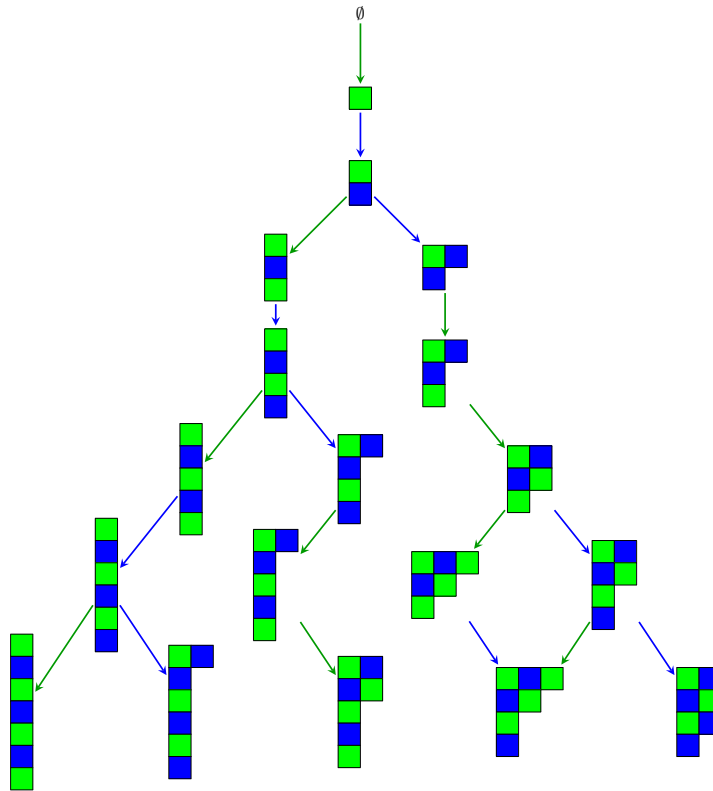


Figure 1: The affine crystal graph $\mathcal{B}_{1,b}^{\mathcal{P}}$

We recall some basic properties of the affine crystal graph $\mathcal{B}_{1,b}^{\mathcal{P}}$ (see [16] or [14, Chapter 10]):

- (i) Every vertex has at least one outgoing edge.
- (ii) Ignoring edge colours, $\mathcal{B}_{1,b}^{\mathcal{P}}$ forms a ranked poset, that is, any two paths from the empty partition to a given vertex have the same length.
- (iii) The rank generating function of this poset is the infinite product $(-q; q)_{\infty}$.

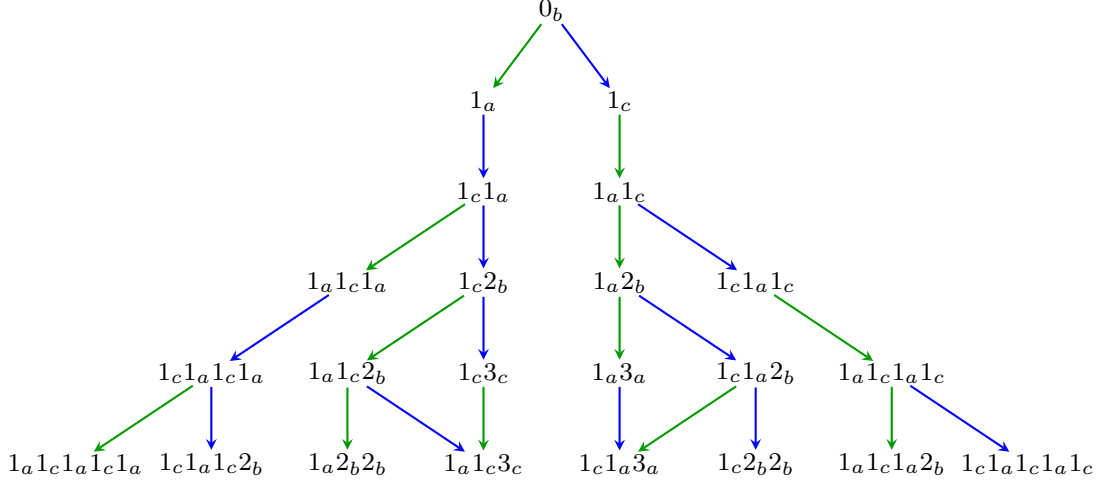


Figure 2: Affine crystal graph of highest weight $\Lambda_0 + \Lambda_1$

The affine crystal graph structure on $\mathcal{P}_{1,b}$ is induced from the graph structure on the set of distinct-part partitions \mathcal{D} via the obvious bijection between $\mathcal{P}_{1,b}$ and \mathcal{D} . The affine crystal graph structure on $\mathcal{P}_{2,b}$ was previously unknown.

In [10], Foda, Leclerc, Okado, Thibon and Welsh described three combinatorial models for the affine crystal graph of type $A_n^{(1)}$ with highest weight $\ell_0\Lambda_0 + \dots + \ell_n\Lambda_n$ for any nonnegative integers ℓ_i and arbitrary rank n . Here we only consider rank $n = 1$ and highest weights $2\Lambda_0$, $\Lambda_0 + \Lambda_1$, and $2\Lambda_1$. We consider the model denoted by $\mathcal{M}(\Lambda)$ in [10], where the set of vertices is a subset of the set of pairs of distinct-part partitions. This model also appears in Geck and Jacon [13, Proposition 6.2.14], and it is known as the *asymptotic model*. Both partitions have a blue–green checkerboard colouring with opposite colours in the top-left corner. Again, contrary to the classical references, the reading order goes from bottom to top.

Another model described in [10], known as the *FLOTW-model*, is the same as the asymptotic model, except that the reading order is not from bottom to top but is instead determined by the contents of the boxes in the diagram. Although the two models are isomorphic, their vertex sets are different. The vertices of the FLOTW-model are known as *Kleshchev multipartitions*. Their crystal-theoretic properties were studied, for example, by Ariki, Kreiman, and Tsuchioka [1], and they were recently studied from a combinatorial perspective by Chern, Li, Stanton, Xue, and Yee [5].

In Section 3, we endow the set $\mathcal{P}_{2,b}$ with an affine crystal graph structure of type $A_1^{(1)}$ and highest weight $\Lambda_0 + \Lambda_1$. The arrows are defined via bracketing rules analogous to those in Definition 1.14, and the construction is obtained through an explicit graph isomorphism with the asymptotic model. The affine crystal graph structure on $\mathcal{P}_{2,b}$ is illustrated in Figure 2. We also construct a new combinatorial model for the affine crystal graphs of highest weight $2\Lambda_0$ (resp. $2\Lambda_1$), type $A_1^{(1)}$, using a slight modification of sets $\mathcal{P}_{2,c}$ (resp. $\mathcal{P}_{2,a}$) as vertices. The classical bracket rule in Theorem 1.14 using addable and removable corners does not generalise to grounded partitions at level 2. In order to do this, we introduce the notion of type.

To study the combinatorics of the affine crystal graphs on $\mathcal{P}_{1,b}$ and $\mathcal{P}_{2,b}$, we consider the following question: what happens when the green (affine) arrows are erased from the affine crystal graph? The infinite connected graph decomposes into an infinite disjoint union of finite blue strings. From the representation-theoretic point of view, this corresponds to the restriction of the representation to the subalgebra \mathfrak{sl}_2 .

To describe the generating functions that arise from this restriction, we need some notation. For integers $n \geq 0$,

the q -integer $[n]_q$ and the q -factorial $[n]_q!$ are defined by

$$[n]_q := 1 + q + \cdots + q^{n-1}, \quad \text{and} \quad [n]_q! := [n]_q [n-1]_q \cdots [1]_q.$$

For two integers $n \geq k \geq 0$, the q -binomial coefficient is

$$\begin{bmatrix} n \\ k \end{bmatrix}_q := \frac{[n]_q!}{[k]_q! [n-k]_q!},$$

and the q -Yamanouchi number $Y_q(n, k)$ is defined by

$$Y_q(n, k) := \frac{[n-k+1]_q}{[n+1]_q} \begin{bmatrix} n+k \\ n \end{bmatrix}_q.$$

Finally, in Section 4, we obtain the following identities: the generating function (1.4) of grounded partitions in $\mathcal{P}_{1,b}$, and the generating function (1.5) of grounded partitions in $\mathcal{P}_{2,b}$, can both be expressed as explicit infinite sums. Remarkably, the generating function of the (modified) major index statistic on Yamanouchi words (see Subsection 4.1) appears in these formulas.

Theorem 1.16. We have

$$\begin{aligned} (-q; q)_\infty &= \sum_{n \geq k \geq 0} q^{n(2n-1)+3k} Y_{q^2}(2n-k, k) (q^2; q^2)_{2n}^{-1} [2(n-k)+1]_q \\ &= \sum_{n \geq k \geq 0} q^{(2n+1)n+3k} Y_{q^2}(2n+1-k, k) (q^2; q^2)_{2n+1}^{-1} [2(n-k)+2]_q. \end{aligned}$$

Theorem 1.17. We have

$$\frac{(-q; q^2)_\infty}{(q; q^2)_\infty} = \sum_{n \geq k \geq 0} q^{2k+(n-k)^2} Y_{q^4}(n, k) (q^2; q^2)_{n+k}^{-1} [2(n-k)+2]_q.$$

The remainder of the paper is organised as follows. In Section 2, we prove Theorems 1.9 and 1.10, thereby showing bijectively that the generating functions (1.5) and (1.6) for grounded partitions at level 2 are infinite products. In Section 3, we construct affine crystal graphs of type $A_1^{(1)}$ and highest weights $2\Lambda_0$, $\Lambda_0 + \Lambda_1$, and $2\Lambda_1$, whose vertices are grounded partitions at level 2. In Section 4, we prove the q -series identities in Theorems 1.16 and 1.17 by decomposing the grounded partition model at levels 1 and 2 into crystal graphs of finite type A_1 .

Acknowledgements

The authors warmly thank Jehanne Dousse for her guidance throughout as well as her valuable comments on the earlier versions of this paper. We are also grateful to Thomas Gerber, Frédéric Jouhet, Christian Krattenthaler, Philippe Nadeau and Ali Uncu for valuable discussions and insightful comments that contributed to the development of this work. The authors are funded by the SNSF Eccellenza grant of Jehanne Dousse, PCEFP2 202784.

2 Bijections at level 2

2.1 Bijection between $\mathcal{P}_{2,b}$ and odd overpartitions

In this subsection, we give two proofs of (1.5). The first is a bijective proof, while the second is a ‘semi-combinatorial’ proof, based on a generating function derived from grounded partitions and the use of hypergeometric series.

We first introduce a combinatorial object corresponding to the right-hand side of (1.5), namely overpartitions into odd parts, and then establish a bijection with grounded partitions in $\mathcal{P}_{2,b}$. An *overpartition*, introduced by Corteel and Lovejoy [6], is a partition where the first occurrence of each number may be overlined. In other words, the overlined parts form a partition into distinct parts and the non-overlined parts form a classical partition.

Let $\overline{\mathcal{P}}$ denote the set of overpartitions. It is well-known [6] that the generating function of overpartitions is given by

$$\sum_{\lambda \in \overline{\mathcal{P}}} q^{|\lambda|} = \frac{(-q; q)_{\infty}}{(q; q)_{\infty}}.$$

We consider overpartitions in which all parts are odd. Let $\overline{\mathcal{PO}}$ denote the set of overpartitions into odd parts. This case is closely related to known results, and the corresponding generating function that keeps track of the length follows readily:

$$\sum_{\lambda \in \overline{\mathcal{PO}}} t^{\ell(\lambda)} q^{|\lambda|} = \frac{(-tq; q^2)_{\infty}}{(tq; q^2)_{\infty}}. \quad (2.1)$$

Example 2.1. We list all grounded partitions in $\mathcal{P}_{2,b}$ of sizes from 0 to 6 in Example 1.7 (iii), which we can compare with the list of all overpartitions into odd parts of the same size for sizes from 0 to 6:

- Size 0: \emptyset
- Size 1: $(1), (\overline{1})$
- Size 2: $(1, 1), (\overline{1}, 1)$
- Size 3: $(1, 1, 1), (\overline{1}, 1, 1), (3), (\overline{3})$
- Size 4: $(1, 1, 1, 1), (\overline{1}, 1, 1, 1), (3, 1), (3, \overline{1}), (\overline{3}, 1), (\overline{3}, \overline{1})$
- Size 5: $(1, 1, 1, 1, 1), (\overline{1}, 1, 1, 1, 1), (3, 1, 1), (3, \overline{1}, 1), (\overline{3}, 1, 1), (\overline{3}, \overline{1}, 1), (5), (\overline{5})$
- Size 6: $(1, 1, 1, 1, 1, 1), (\overline{1}, 1, 1, 1, 1, 1), (3, 1, 1, 1), (3, \overline{1}, 1, 1), (\overline{3}, 1, 1, 1), (\overline{3}, \overline{1}, 1, 1), (3, 3), (\overline{3}, 3), (5, 1), (5, \overline{1}), (\overline{5}, 1), (\overline{5}, \overline{1})$

We seek a size-preserving bijection between these sets. A more refined version, which also fixes the number of odd parts, is not only easier to construct but also yields a stronger result.

Example 2.2. We list all 20 partitions in $\mathcal{P}_{2,b}$ of size 11 having 3 odd parts:

$$\begin{aligned} &1_a 1_c 1_a 2_b 2_b 2_b 2_b, \quad 1_c 1_a 1_c 2_b 2_b 2_b 2_b, \quad 1_a 1_c 2_b 2_b 2_b 3_a, \quad 1_a 1_c 2_b 2_b 2_b 3_c, \\ &1_c 1_a 2_b 2_b 2_b 3_a, \quad 1_c 1_a 2_b 2_b 2_b 3_c, \quad 1_a 2_b 2_b 3_a 3_c, \quad 1_a 2_b 2_b 3_c 3_a, \\ &1_c 2_b 2_b 3_a 3_c, \quad 1_c 2_b 2_b 3_c 3_a, \quad 1_a 3_a 3_c 4_b, \quad 1_c 3_c 3_a 4_b, \\ &1_a 1_c 2_b 3_a 4_b, \quad 1_a 1_c 2_b 3_c 4_b, \quad 1_c 1_a 2_b 3_a 4_b, \quad 1_c 1_a 2_b 3_c 4_b, \\ &1_a 2_b 3_a 5_a, \quad 1_a 2_b 3_c 5_c, \quad 1_c 2_b 3_a 5_a, \quad 1_c 2_b 3_c 5_c, \end{aligned}$$

as well as all 20 overpartitions into odd parts of size 11 and length 3:

$$\begin{aligned} &(9, 1, 1), (9, \overline{1}, 1), (\overline{9}, 1, 1), (\overline{9}, \overline{1}, 1), (7, 3, 1), \\ &(7, 3, \overline{1}), (7, \overline{3}, 1), (\overline{7}, 3, 1), (7, \overline{3}, \overline{1}), (\overline{7}, 3, \overline{1}), \\ &(\overline{7}, \overline{3}, 1), (\overline{7}, \overline{3}, \overline{1}), (5, 5, 1), (5, 5, \overline{1}), (\overline{5}, 5, 1), \\ &(\overline{5}, 5, \overline{1}), (5, 3, 3), (5, \overline{3}, 3), (\overline{5}, 3, 3), (\overline{5}, \overline{3}, 3). \end{aligned}$$

We begin by observing the grounded partitions in $\mathcal{P}_{2,b}$. All even parts are coloured b . Consider an odd part $2i + 1$. If $2i$ appears in the grounded partition, then the first $2i + 1$ can be coloured either a or c ; otherwise, the first $2i + 1$ has the same colour as that of the last part $2i - 1$. Once the colour of the first occurrence of an odd part is chosen, the colours of all other parts of the same size alternate between a and c . Even parts may or may not appear, but each odd part must appear at least once. The following bijection is the main result of this subsection, and is stated in Theorem 1.9.

Theorem 2.3. Let $\mathcal{P}_b(n, k)$ denote the set of grounded partitions in $\mathcal{P}_{2,b}$ of size n with k odd parts, and let $\overline{\mathcal{PO}}(n, k)$ denote the set of overpartitions into odd parts of size n and length k . Then, for all integers $n \geq k \geq 0$, there is a bijection between $\mathcal{P}_b(n, k)$ and $\overline{\mathcal{PO}}(n, k)$. In particular, we have

$$|\mathcal{P}_b(n, k)| = |\overline{\mathcal{PO}}(n, k)|.$$

Proof. We prove this theorem by providing a bijection between the two sets. We begin by defining a map from $\mathcal{P}_b(n, k)$ to $\overline{\mathcal{PO}}(n, k)$. The idea is to add the even parts to the odd parts of the grounded partitions in such a way that the colour sequence of the odd parts remains unchanged, not only the number of odd parts.

Step 1: Given a grounded partition $\pi \in \mathcal{P}_b(n, k)$, we first define the corresponding *minimal grounded partition* $\pi_{\min} \in \mathcal{P}_{2,b}$ with k odd parts as follows. We remove as many even parts as possible from π , such that the resulting partition still belongs to $\mathcal{P}_b(n, k)$. More explicitly, suppose that at least one even part $(2i)_b$ appears between two consecutive odd parts, namely $(2i - 1)_x(2i)_b \cdots (2i)_b(2i + 1)_y$, where $x, y \in \{a, c\}$. If the two odd parts have the same colour, that is, $x = y = a$ or $x = y = c$, then all such even parts are removed, because $(2i - 1)_x(2i + 1)_y$ still satisfies the difference conditions of M_2 . If they have different colours, namely $(x, y) = (a, c)$ or (c, a) , then all but one even part $(2i)_b$ are removed, because $(2i - 1)_x(2i + 1)_y$ does not satisfy the difference conditions but $(2i - 1)_x(2i)_b(2i + 1)_y$ does. We denote the resulting grounded partition by π_{\min} , and the partition consisting of the removed even parts by π_e , where we also removed the colour b from the parts. We call the even parts removed from π the *loose parts*. This step is illustrated in Figure 3.

$$\underbrace{1_c 1_a 1_c 2_b 2_b 3_a 3_c 5_c 5_a 6_b 6_b 7_a 7_c 7_a 7_c 8_b 9_a}_{\pi} \mapsto \left(\underbrace{1_c 1_a 1_c 2_b 3_a 3_c 5_c 5_a 7_a 7_c 7_a 7_c 8_b 9_a}_{\pi_{\min}}, \underbrace{(2, 6, 6)}_{\pi_e} \right)$$

Figure 3: From grounded partition to overpartition: step 1

Step 2: Using π_{\min} and π_e , we construct an overpartition into odd parts. For each even part $2i$ in π_{\min} , starting from the smallest, we increase the i odd parts to the left of $2i$ by 2. By definition of $\mathcal{P}_{2,b}$, each odd part between 1 and $2i - 1$ must appear at least once, so there are at least i odd parts to the left of $2i$. Let $\pi^{(1)}$ be the resulting partition. Note that all parts of $\pi^{(1)}$ are odd, though $\pi^{(1)}$ may no longer belong to $\mathcal{P}_{2,b}$. This step is illustrated in Figure 4.

$$\left(\underbrace{1_c 1_a 1_c 2_b 3_a 3_c 5_c 5_a 7_a 7_c 7_a 7_c 8_b 9_a}_{\pi_{\min}}, \underbrace{(2, 6, 6)}_{\pi_e} \right) \mapsto \left(\underbrace{1_c 1_a 3_c 3_a 3_c 5_c 5_a 9_a 9_c 9_a 9_c 9_a}_{\pi^{(1)}}, \underbrace{(2, 6, 6)}_{\pi_e} \right)$$

Figure 4: From grounded partition to overpartition: step 2

Step 3: We now proceed to add the parts of π_e to those of $\pi^{(1)}$. For each even part $2i$ in π_e , we increase the

largest i odd parts of $\pi^{(1)}$ by 2 (the order of increasing these parts does not matter). Let $\pi^{(2)}$ denote the resulting coloured partition. This step is illustrated in Figure 5.

$$\left(\underbrace{1_c 1_a 3_c 3_a 3_c 5_c 5_a 9_c 9_a 9_c 9_a}_{\pi^{(1)}}, \underbrace{(2, 6, 6)}_{\pi_e} \right) \mapsto \underbrace{1_c 1_a 3_c 3_a 3_c 5_c 5_a 9_c 9_a 13_a 13_c 15_a}_{\pi^{(2)}}$$

Figure 5: From grounded partition to overpartition: step 3

Step 4: Finally, for the first occurrence of each value in $\pi^{(2)}$, we place a bar when its colour is c , and leave it unbarred when its colour is a . By removing all colours from $\pi^{(2)}$, we obtain an overpartition into odd parts of length k from $\pi^{(2)}$. This final step is illustrated in Figure 6.

$$\underbrace{1_c 1_a 3_c 3_a 3_c 5_c 5_a 9_c 9_a 13_a 13_c 15_a}_{\pi^{(2)}} \mapsto \underbrace{(\bar{1}, 1, \bar{3}, 3, 3, \bar{5}, 5, 9, 9, 13, 13, 15)}_{\lambda}$$

Figure 6: From grounded partition to overpartition: step 4

Inverse map, Step 1: We now define a map from $\overline{\mathcal{PO}}(n, k)$ to $\mathcal{P}_b(n, k)$, which is the inverse of the map defined above. Let $\lambda = (\lambda_1 \leq \dots \leq \lambda_k)$ be an overpartition into odd parts of length k . From λ , we first construct a grounded partition π_s with only odd parts and a specified colour sequence. For a maximal sequence $\lambda_i = \dots = \lambda_j$ with $i \leq j$ of equal parts, we assign colour a to the part λ_i if it is unbarred, and c if it is barred. The remaining parts $\lambda_{i+1}, \dots, \lambda_j$ are coloured alternately in a and c . This gives a colour sequence (s_1, \dots, s_k) , where λ_i is coloured s_i . There is a unique grounded partition $\pi_s \in \mathcal{P}_{2,b}$ with this colour sequence. Indeed, the first part is not coloured b , and afterwards repeated colours increase the part size by two, while alternating colours leave the size unchanged. This step is illustrated in Figure 7.

$$\underbrace{(\bar{1}, 1, \bar{3}, 3, 3, \bar{5}, 5, 9, 9, 13, 13, 15)}_{\lambda} \mapsto \underbrace{ca cac ca ac ac a}_{(s_1, \dots, s_k)} \mapsto \underbrace{1_c 1_a 1_c 1_a 1_c 3_c 3_a 5_a 5_c 5_a 5_c 5_a}_{\pi_s}$$

Figure 7: From overpartition to grounded partition: step 1

Step 2: We construct an array of $2s$ beneath the grounded partition π_s , arranged so that the sum of each column gives the corresponding part of the original overpartition λ . This array encodes how much each odd part in π_s must be increased by to reconstruct λ . See Figure 8.

Step 3: This is a recursive construction. At each iteration, let m be the number of columns in the array of $2s$, and let $2j - 1$ be the largest part in the current partition. In Figure 8, we have $m = 10$ and $j = 3$.

- (i) First, assume $m > j$. We insert a non-loose even part into the grounded partition. There exists a unique gap between parts $(2i - 1)_x$ and $(2i - 1)_y$ with $(x, y) = (a, c)$ or (c, a) , such that the number of $2s$ in the top row of the array—read from the left up to and including the column below $(2i - 1)_a$ —is exactly i . Indeed, the number of $2s$ up to and including the largest odd part of size $2j - 1$ is at least j , while the number of $2s$

The first map is clearly reversible. By the construction of the inverse map, one can easily see that the second map is also reversible. Since the two maps in the process are reversible, the two sets $\mathcal{P}_b(n, k)$ and $\overline{\mathcal{PO}}(n, k)$ are in bijection, which completes the proof. \square

By Theorem 2.3 and the generating function (2.1) with $t = 1$, we arrive at a bijective proof of (1.5). For a grounded partition π , let $odd(\pi)$ denote the number of odd parts in π . Then we obtain the following bivariate generating function:

Lemma 2.4. We have

$$\sum_{\pi \in \mathcal{P}_{2,b}} t^{odd(\pi)} q^{|\pi|} = \sum_{n \geq 0} \frac{t^n q^{n^2} (-1; q^2)_n}{(tq; q^2)_n (q^2; q^2)_n}.$$

Proof. Let $2n - 1$ be the largest odd part of $\pi \in \mathcal{P}_{2,b}$. Then each odd part $1, 3, \dots, 2n - 1$ appears at least once, contributing the factor $t^n q^{n^2} / (tq; q^2)_n$ without keeping track of the colours.

In a grounded partition $\pi \in \mathcal{P}_{2,b}$, all even parts are coloured b , and all odd parts are coloured a or c , alternatingly along each number $2i + 1$ for $1 \leq i \leq n$. Thus the colour of the first occurrence of $2i + 1$ determines the colour of all parts $2i + 1$. One can encode the colour of the first $2i + 1$ by overlining or leaving unbarred the preceding even number $2i$ (whether or not it appears as a part). This contributes the factor $(-1; q^2)_n$. The even parts in π are generated by $1/(q^2; q^2)_n$, without keeping track of the colours. Combining these contributions yields the desired generating function. \square

Using the previous results, we obtain the following q -series identity, stated in Theorem 1.11. This identity can also be proved analytically using hypergeometric series. We provide both proofs.

Theorem 2.5. We have

$$\sum_{n \geq 0} \frac{t^n q^{n^2} (-1; q^2)_n}{(tq; q^2)_n (q^2; q^2)_n} = \frac{(-tq; q^2)_\infty}{(tq; q^2)_\infty}.$$

First proof. This follows from the generating functions for two partition models in Lemma 2.4 and (2.1), together with the bijection between the two models in Theorem 2.3. \square

Second proof. We begin with Heine's q -analogue of Gauss' summation formula [12, (1.5.1)]:

$${}_2\phi_1(a, b; c; q, c/ab) := \sum_{n \geq 0} \frac{(a; q)_n (b; q)_n}{(q; q)_n (c; q)_n} (c/ab)^n = \frac{(c/a; q)_\infty (c/b; q)_\infty}{(c; q)_\infty (c/ab; q)_\infty}. \quad (2.2)$$

Letting $b \rightarrow \infty$, we obtain the following limiting case of (2.2):

$$\sum_{n \geq 0} \frac{(-1)^n c^n q^{n(n-1)/2} (a; q)_n}{a^n (q; q)_n (c; q)_n} = \frac{(c/a; q)_\infty}{(c; q)_\infty}. \quad (2.3)$$

This identity also appears in [25, Theorem 1.75].

The left-hand side can be rewritten as

$$\sum_{n \geq 0} \frac{t^n q^{n^2} (-1; q^2)_n}{(tq; q^2)_n (q^2; q^2)_n} = \sum_{n \geq 0} \frac{(-1)^n (tq)^n (q^2)^{n(n-1)/2} (-1; q^2)_n}{(-1)^n (q^2; q^2)_n (tq; q^2)_n}.$$

The proof follows from (2.3) by substituting $q \mapsto q^2$, and then $a = -1$ and $c = tq$. \square

Without using our bijection in Theorem 2.3, Equation (1.5) can also be derived from the infinite sum expression of the generating function for grounded partitions in Lemma 2.4 and the q -series identity in Theorem 2.5 proved via hypergeometric series. This provides the semi-combinatorial proof of (1.5).

The infinite product expression for the right-hand side of (1.5) follows immediately by substituting $t = 1$ in Theorem 2.5. We conclude this subsection with the following corollary.

Corollary 2.6. We have

$$\sum_{n \geq 0} \frac{q^{n^2} (-1; q^2)_n}{(q; q)_{2n}} = \frac{(-q; q^2)_\infty}{(q; q^2)_\infty}.$$

2.2 Bijection between $\mathcal{P}_{2,a}$ and partitions without repeating even parts

In this subsection we provide a bijective proof of (1.6), as well as a semi-combinatorial proof using hypergeometric series. The right-hand side of (1.6) is the generating function of partitions where even parts do not repeat. Apart from this distinction, the overall structure of this subsection follows that of Subsection 2.1.

Let \mathcal{E} denote the set of partitions where all even parts are distinct. Then, we have

$$\sum_{\lambda \in \mathcal{E}} t^{\text{odd}(\lambda)} q^{|\lambda|} = \frac{(-q^2; q^2)_\infty}{(tq; q^2)_\infty}. \quad (2.4)$$

Example 2.7. We list all grounded partitions in $\mathcal{P}_{2,a}$ of sizes from 0 to 6 in Example 1.7 (iv), which we can compare with the list of all partitions in \mathcal{E} of sizes from 0 to 6:

- Size 0: \emptyset
- Size 1: (1)
- Size 2: (1, 1), (2)
- Size 3: (1, 1, 1), (2, 1), (3)
- Size 4: (1, 1, 1, 1), (2, 1, 1), (3, 1), (4)
- Size 5: (1, 1, 1, 1, 1), (2, 1, 1, 1), (3, 1, 1), (3, 2), (4, 1), (5),
- Size 6: (1, 1, 1, 1, 1, 1), (2, 1, 1, 1, 1), (3, 1, 1, 1), (3, 2, 1), (3, 3), (4, 1, 1),
(4, 2), (5, 1), (6)

Remark 2.8. There are many different ways to write the product side in terms of q -Pochhammer symbols. For example, we have:

$$\frac{(-q^2; q^2)_\infty}{(q; q^2)_\infty} = \frac{(q^4; q^4)_\infty}{(q; q)_\infty}.$$

The right-hand side is the generating function for partitions with no part divisible by 4. It seems to us that the product on the left-hand side is more convenient for finding a bijection.

Once again, we can refine this bijection by restricting to a fixed number of odd parts on both sides. We list all

25 partitions in $\mathcal{P}_{2,a}$ of size 14 and 2 odd parts:

$$\begin{aligned}
& 1_b 1_b 2_a 2_c 2_a 2_c 2_a 2_c, \quad 1_b 1_b 2_c 2_a 2_c 2_a 2_c 2_a, \quad 1_b 2_a 2_c 2_a 2_c 2_a 3_b, \quad 1_b 2_c 2_a 2_c 2_a 2_c 3_b, \\
& 1_b 1_b 2_a 2_c 2_a 2_c 4_c, \quad 1_b 1_b 2_c 2_a 2_c 2_a 4_a, \quad 1_b 1_b 2_a 2_c 4_c 4_a, \quad 1_b 1_b 2_c 2_a 4_a 4_c, \\
& 1_b 2_a 2_c 2_a 3_b 4_a, \quad 1_b 2_a 2_c 2_a 3_b 4_c, \quad 1_b 2_c 2_a 2_c 3_b 4_a, \quad 1_b 2_c 2_a 2_c 3_b 4_c, \\
& 1_b 2_a 3_b 4_a 4_c, \quad 1_b 2_c 3_a 4_a 4_c, \quad 1_b 2_a 3_b 4_c 4_a, \quad 1_b 2_c 3_b 4_c 4_a, \\
& 1_b 2_a 2_c 4_c 5_b, \quad 1_b 2_c 2_a 4_a 5_b, \quad 1_b 1_b 2_a 4_a 6_a, \quad 1_b 1_b 2_c 4_c 6_c, \\
& 2_a 2_c 2_a 2_c 3_b 3_b, \quad 2_a 2_c 3_b 3_b 4_a, \quad 2_a 2_c 3_b 3_b 4_c, \quad 2_a 3_b 4_a 5_b, \quad 2_a 3_b 4_c 5_b.
\end{aligned}$$

as well as all 25 partitions in \mathcal{E} of size 14 and 2 odd parts:

$$\begin{aligned}
& (13, 1), (12, 1, 1), (11, 3), (11, 2, 1), (10, 3, 1), \\
& (10, 2, 1, 1), (9, 5), (9, 4, 1), (9, 3, 2), (8, 5, 1), \\
& (8, 4, 1, 1), (8, 3, 3), (8, 3, 2, 1), (7, 7), (7, 6, 1), \\
& (7, 5, 2), (7, 4, 3), (7, 4, 2, 1), (6, 5, 3), (6, 5, 2, 1), \\
& (6, 4, 3, 1), (6, 4, 2, 1, 1), (6, 3, 3, 2), (5, 5, 4), (5, 4, 3, 2).
\end{aligned}$$

In $\mathcal{P}_{2,a}$, all odd parts have colour b , (unlike in $\mathcal{P}_{2,b}$). An even part $2i$ can be coloured either a or c if the part $2i - 1$ appears in the partition. If not, then the first occurrence of $2i$ has the same colour as the colour of the last $2i - 2$. Afterwards, the colours of all parts of size $2i$ alternate a and c . Odd parts may or may not appear, but each even part must appear at least once. The main result of this subsection is the following bijection, stated in Theorem 1.10.

Theorem 2.9. Let $\mathcal{P}_a(n, k)$ denote the set of grounded partitions in $\mathcal{P}_{2,a}$ of size n with k odd parts, and let $\mathcal{E}(n, k)$ denote the set of partitions of size n with k odd parts such that all even parts are distinct. Then, for all integers $n \geq k \geq 0$, there is a bijection between $\mathcal{P}_a(n, k)$ and $\mathcal{E}(n, k)$. In particular, we have

$$|\mathcal{P}_a(n, k)| = |\mathcal{E}(n, k)|.$$

Proof. A modification of the bijective proof of Theorem 2.3 works.

Step 1: The first step is a notational trick. Let $\pi \in \mathcal{P}_a(n, k)$. If an even part $2k$ in π with colour c follows an odd part $2k - 1$, we put a bar over it. If an even part $2k$ with colour a follows an odd part $2k - 1$, we leave it unbarred. Furthermore, whenever there are two consecutive parts $2k$ and $2k + 2$ in π , we put a bar over the first occurrence of $2k + 2$. Finally, we remove the colours to obtain an overpartition $\tilde{\pi}$. We denote the set $\{\tilde{\pi} : \pi \in \mathcal{P}_a(n, k)\}$ by $\tilde{\mathcal{P}}_a(n, k)$, which can be characterised as follows. $\tilde{\mathcal{P}}_a(n, k)$ is the set of overpartitions of size n with k odd parts, where the difference between consecutive parts is 0, 1, or 2; the difference between consecutive odd parts is 0; only even parts can be overlined; and the first occurrence of an even number is overlined if and only if the preceding part is not odd. The map $\pi \mapsto \tilde{\pi}$ is a bijection from $\mathcal{P}_a(n, k)$ to $\tilde{\mathcal{P}}_a(n, k)$. This step is illustrated in Figure 11: we list all partitions in $\tilde{\mathcal{P}}_a(14, 2)$.

$$\begin{aligned}
& (1, 1, 2, 2, 2, 2, 2) \quad (1, 1, \bar{2}, 2, 2, 2, 2) \quad (1, 2, 2, 2, 2, 2, 3), \quad (1, \bar{2}, 2, 2, 2, 2, 3), \\
& (1, 1, 2, 2, 2, 2, \bar{4}), \quad (1, 1, \bar{2}, 2, 2, 2, \bar{4}), \quad (1, 1, 2, 2, \bar{4}, 4), \quad (1, 1, \bar{2}, 2, \bar{4}, 4), \\
& (1, 2, 2, 2, 3, 4), \quad (1, 2, 2, 2, 3, \bar{4}), \quad (1, \bar{2}, 2, 2, 3, 4), \quad (1, \bar{2}, 2, 2, 3, \bar{2}), \\
& (1, 2, 3, 4, 4), \quad (1, \bar{2}, 3, 4, 4), \quad (1, 2, 3, \bar{4}, 4), \quad (1, \bar{2}, 3, \bar{4}, 4), \\
& (1, 2, 2, \bar{4}, 5), \quad (1, \bar{2}, 2, \bar{4}, 5), \quad (1, 1, 2, \bar{4}, \bar{6}), \quad (1, \bar{2}, \bar{4}, \bar{6}), \\
& (\bar{2}, 2, 2, 2, 3, 3), \quad (\bar{2}, 2, 3, 3, 4), \quad (\bar{2}, 2, 3, 3, \bar{4}), \quad (\bar{2}, 3, 4, 5), \quad (\bar{2}, 3, \bar{4}, 5).
\end{aligned}$$

Figure 11: From $\mathcal{P}_a(n, k)$ to $\mathcal{E}(n, k)$: step 1

Step 2: The role of the odd parts in the proof of Theorem 2.3 is replaced by odd parts and barred even parts. Take a partition $\pi \in \mathcal{P}_a(n, k)$ and let $\tilde{\pi} \in \tilde{\mathcal{P}}_a(n, k)$ be the corresponding overpartition. Define the *minimal overpartition* $\pi_{\min} \in \tilde{\mathcal{P}}_a(n, k)$, to be overpartition obtained from $\tilde{\pi}$ by removing as many unbarred even parts as possible while still remaining in $\tilde{\mathcal{P}}_a(n, k)$. As before, we call the even parts removed from $\tilde{\pi}$ the *loose parts*, and denote by π_e the partition consisting of the loose parts. This step is illustrated in Figure 12.

$$\underbrace{(1, 1, 1, \bar{2}, 2, 2, \bar{4}, 4, \bar{6}, 7, 7, 7, 8, 8, 9, 9, 10, 11)}_{\pi} \mapsto \left(\underbrace{(1, 1, 1, \bar{2}, \bar{4}, \bar{6}, 7, 7, 7, 8, 9, 9, 10, 11)}_{\pi_{\min}}, \underbrace{(2, 2, 4, 8)}_{\pi_e} \right)$$

Figure 12: From $\mathcal{P}_a(n, k)$ to $\mathcal{E}(n, k)$: step 2

Step 3: This step is analogous to Step 2 of the forward direction of the proof in Theorem 2.3. For each unbarred even part $2i$ in π_{\min} , starting from the smallest, we add 2 to the i odd or barred even parts that precede it. Again, by definition of $\tilde{\mathcal{P}}_a(n, k)$, there are always at least i such odd or barred even parts. We repeat this process until no unbarred even parts remain, and call the resulting partition $\pi^{(1)}$. This step is illustrated in Figure 13.

$$\left(\underbrace{(1 \quad 1 \quad 1 \quad \bar{2} \quad \bar{4} \quad \bar{6} \quad 7 \quad 7 \quad 7 \quad 8 \quad 9 \quad 9 \quad 10 \quad 11)}_{\pi_{\min}}, \underbrace{(2, 2, 4, 8)}_{\pi_e} \right) \mapsto \left(\underbrace{(1, 1, 1, \bar{2}, \bar{4}, \bar{8}, 11, 11, 11, 11, 11, 11)}_{\pi^{(1)}}, \underbrace{(2, 2, 4, 8)}_{\pi_e} \right)$$

Figure 13: From $\mathcal{P}_a(n, k)$ to $\mathcal{E}(n, k)$: step 3

Step 4: We construct the overpartition $\pi^{(2)}$ from $\pi^{(1)}$ and π_e , as before. For each part $2i$ in π_e , starting from the largest, we add 2 to the largest i odd or barred even parts in $\pi^{(1)}$. Repeating this process yields an overpartition $\pi^{(2)}$ of the same size as π . This step is illustrated in Figure 14.

$$\left(\underbrace{(1, 1, 1, \bar{2}, \bar{4}, \bar{8}, 11, 11, 11, 11, 11, 11)}_{\pi^{(1)}}, \underbrace{(2, 2, 4, 8)}_{\pi_e} \right) \mapsto \underbrace{(1, 1, 1, \bar{2}, \bar{4}, \bar{8}, 11, 11, 13, 13, 15, 19)}_{\pi^{(2)}}$$

Figure 14: From $\mathcal{P}_a(n, k)$ to $\mathcal{E}(n, k)$: step 4

Finally, we obtain λ in $\mathcal{E}(n, k)$ from $\pi^{(2)}$ by removing all bars from its (distinct) even parts.

The construction of the inverse map is similar to the inverse map in the proof of Theorem 2.3.

Inverse map, Step 1: Let $\lambda = (\lambda_1 \leq \dots \leq \lambda_\ell)$ be a partition in $\mathcal{E}(n, k)$. We construct an overpartition λ_s from λ as follows. If λ_1 is odd, then $(\lambda_s)_1 = 1$; if λ_1 is even, then $(\lambda_s)_1 = 2$. For $1 \leq i \leq \ell - 1$, if λ_i and λ_{i+1} are both odd, then $(\lambda_s)_{i+1} = (\lambda_s)_i$; if λ_i and λ_{i+1} have different parity, then $(\lambda_s)_{i+1} = (\lambda_s)_i + 1$; if λ_i and λ_{i+1} are both even, then $(\lambda_s)_{i+1} = (\lambda_s)_i + 2$. After determining all sizes of parts of λ_s , we place a bar on every even part to complete the construction. This step is illustrated in Figure 15.

$$(1, 1, 1, 2, 4, 8, 11, 11, 13, 13, 15, 19) \mapsto (1, 1, 1, \bar{2}, \bar{4}, \bar{6}, 7, 7, 7, 7, 7, 7)$$

Figure 15: From $\mathcal{E}(n, k)$ to $\mathcal{P}_a(n, k)$: step 1

Step 2: We construct an array of 2s beneath the overpartition λ_s , arranged so that the sum of each column gives the corresponding part of the original overpartition λ . This array encodes how much each odd or overlined even part in λ_s must be increased by to reconstruct λ . See Figure 16.

$$(1, 1, 1, 2, 4, 8, 11, 11, 13, 13, 15, 19) \mapsto \begin{array}{cccccccccccc} 1 & 1 & 1 & \bar{2} & \bar{4} & \bar{6} & 7 & 7 & 7 & 7 & 7 & 7 \\ & & & & & & 2 & 2 & 2 & 2 & 2 & 2 \\ & & & & & & & 2 & 2 & 2 & 2 & 2 \\ & & & & & & & & 2 & 2 & 2 & 2 \\ & & & & & & & & & 2 & 2 & \\ & & & & & & & & & & 2 & \\ & & & & & & & & & & & 2 \\ & & & & & & & & & & & & 2 \end{array}$$

Figure 16: From $\mathcal{E}(n, k)$ to $\mathcal{P}_a(n, k)$: step 2

Step 3: This is a recursive construction. At each iteration, let m be the number of columns in the array of 2s, and let $2j - 1$ be the largest part in the current partition. In Figure 16, we have $m = 7$ and $j = 4$. We omit the detailed description of this recursive construction, as it is completely analogous to the map in Step 3 of the inverse map in the proof of Theorem 2.3. The inserted non-loose even parts are unbarred. The two iterations in our running examples are illustrated in Figures 17 and 18. From this procedure, we obtain the pair (π_{\min}, π_e) , where π_{\min} is the overpartition in the top row, and π_e is the partition whose parts are given by the row sums of the remaining array of 2s.

$$\mapsto \begin{array}{cccccccccccc} 1 & 1 & 1 & \bar{2} & \bar{4} & \bar{6} & 7 & 7 & 7 & 8 & 9 & 9 & 9 \\ & & & & & & 2 & 2 & 2 & & 2 & 2 & 2 \\ & & & & & & & 2 & & 2 & 2 & 2 & \\ & & & & & & & & & & 2 & 2 & \\ & & & & & & & & & & & 2 & \\ & & & & & & & & & & & & 2 \end{array}$$

Figure 17: From $\mathcal{E}(n, k)$ to $\mathcal{P}_a(n, k)$: step 3, first iteration

Second proof. The proof is similar to the second proof of Theorem 2.5. By taking $q \mapsto q^2$, and then substituting $a = -tq$ and $c = tq^3$ into (2.3), we have

$$\sum_{n \geq 0} \frac{q^{n^2+n}(-tq; q^2)_n}{(q^2; q^2)_n(tq^3; q^2)_n} = \frac{(-q^2; q)_\infty}{(tq^3; q)_\infty}.$$

Multiplying both sides by $1/(1 - tq)$ completes the proof. □

Corollary 2.12. We have

$$\sum_{n \geq 0} \frac{q^{n(n+1)}(-q; q^2)_n}{(q; q)_{2n+1}} = \frac{(-q^2; q^2)_\infty}{(q; q^2)_\infty}.$$

3 Affine crystal graphs on grounded partitions at level 2

In this section, we construct affine crystal graphs of type $A_1^{(1)}$ and highest weights $2\Lambda_0$, $\Lambda_0 + \Lambda_1$, and $2\Lambda_1$, whose vertices are grounded partitions at level 2. We first define directed graphs on grounded partitions, illustrated in Figure 2. We then prove that these are isomorphic to the affine crystal graphs of type $A_1^{(1)}$ given by the asymptotic model, shown in Figure 20. The proofs are given by constructing explicit graph isomorphisms.

First, we reformulate the description of the affine crystal graph $\mathcal{P}_{1,b}$ in Definition 1.14. In Remark 3.9, we explain why this modification is necessary, to define an affine crystal graph on $\mathcal{P}_{2,b}$.

Definition 3.1. Consider the blue–green checkerboard pattern on Young diagrams. The top-left cell may be either green or blue. We define the *type* of a partition λ , denoted $\text{type}(\lambda)$, to be the binary word constructed as follows. Read the columns from left to right and look at the bottom cell of each column: assign 0 if it is green, and assign 1 if it is blue. If the first row of λ ends in green, append an additional 0 at the end.

For the empty partition \emptyset , we set $\text{type}(\emptyset) := 0$ if the top-left cell is green, and $\text{type}(\emptyset) := \emptyset$ if the top-left cell is blue.

Example 3.2. A few examples of conjugate distinct-part partitions and their types, with the top-left cell green, are shown in Figure 19. For a conjugate distinct-part partition λ , each column has a removable or addable blue corner. Consequently, the sequence of brackets associated to $\text{type}(\lambda)$ is the same as the sequence of brackets obtained from addable and removable blue corners of λ according to Definition 1.14.

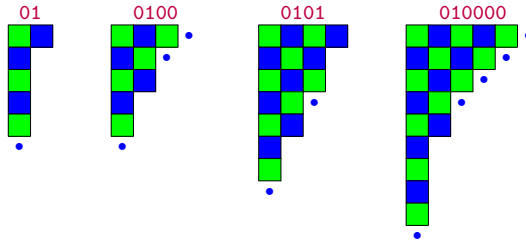


Figure 19: Partitions and the their types

Definition 3.3. The directed graph $\mathcal{B}_{1,b}^{\mathcal{P}}$, whose vertices are partitions and whose edges are coloured blue and green, is defined recursively starting from the empty partition \emptyset . For each vertex λ , consider the blue–green checkerboard where the top-left cell is green. The outgoing arrows are determined by the following bracketing rules:

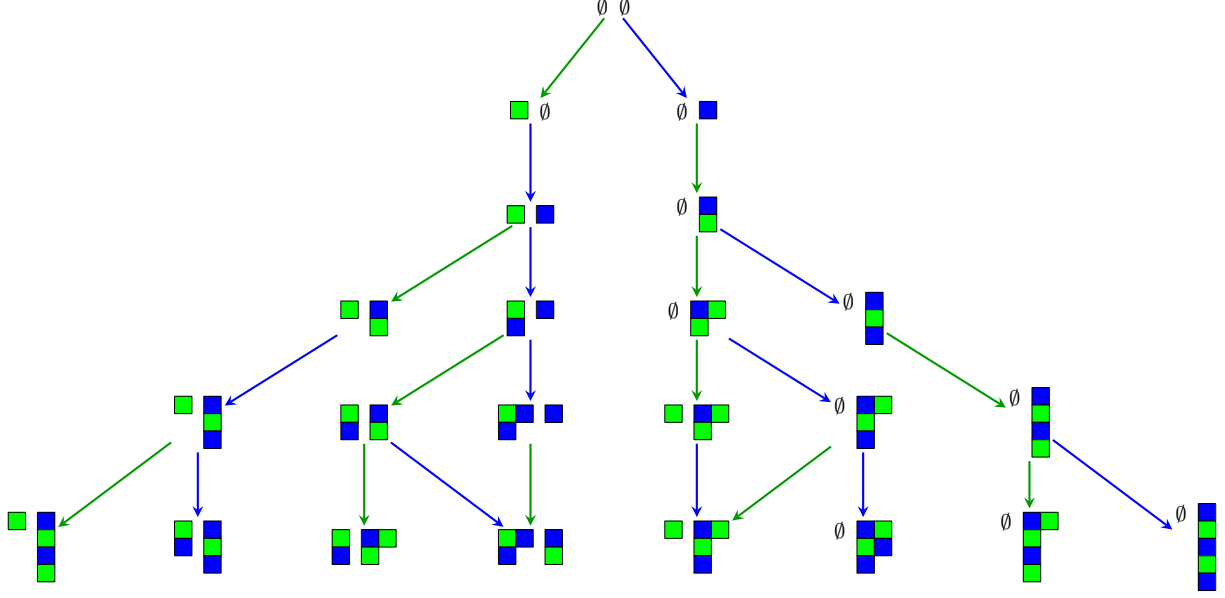


Figure 20: The graph $\mathcal{B}_{2,b}^A$

- (i) **Blue arrow.** Assign a left bracket “(” to each 0 in $\text{type}(\lambda)$, and a right bracket “)” to each 1. Take the leftmost unmatched 0, and add a blue cell at the bottom of the corresponding column of λ . A blue arrow is drawn from λ to the resulting partition.
- (ii) **Green arrow.** Defined in the same way, using the binary word obtained by interchanging the roles of blue and green cells in the definition of $\text{type}(\lambda)$.

As mentioned below Definition 1.14, the vertex set of the graph $\mathcal{B}_{1,b}^P$ is the set of conjugate distinct-part partitions.

Definition 3.4. Consider pairs of partitions $(\lambda^{(1)}, \lambda^{(2)})$, where $\lambda^{(1)}$ is coloured in a blue–green checkerboard pattern with the top-left cell green, and $\lambda^{(2)}$ is coloured in the same way but with the top-left cell blue. We define the *type* of the pair $(\lambda^{(1)}, \lambda^{(2)})$, denoted $\text{type}(\lambda^{(1)}, \lambda^{(2)})$, to be the binary word obtained by concatenating $\text{type}(\lambda^{(2)})$ and $\text{type}(\lambda^{(1)})$:

$$\text{type}(\lambda^{(1)}, \lambda^{(2)}) := \text{type}(\lambda^{(2)}) \text{type}(\lambda^{(1)}).$$

The directed graph $\mathcal{B}_{2,b}^A$, whose vertices are pairs of partitions and whose edges are coloured blue and green, is defined recursively starting from the empty pair $(\lambda^{(1)}, \lambda^{(2)}) = (\emptyset, \emptyset)$. For each vertex $(\lambda^{(1)}, \lambda^{(2)})$, the outgoing arrows are determined by the following bracketing rules:

- (i) **Blue arrow.** Assign a left bracket “(” to each letter 0 in $\text{type}(\lambda^{(1)}, \lambda^{(2)})$, and a right bracket “)” to each 1. Take the leftmost unmatched 0, and add a blue cell at the bottom of the corresponding column of $\lambda^{(1)}$ or $\lambda^{(2)}$. A blue arrow is drawn from $(\lambda^{(1)}, \lambda^{(2)})$ to the resulting pair of partitions.
- (ii) **Green arrow.** Defined in the same way, using the binary word obtained by interchanging the roles of blue and green cells in the definition of $\text{type}(\lambda^{(1)}, \lambda^{(2)})$.

Remark 3.5. (i) It follows from the signature rule [3, Section 2.4] for the tensor product of crystals that the graph $\mathcal{B}_{2,b}^A$ is isomorphic to a connected component of the tensor product $\mathcal{B}(\Lambda_0) \otimes \mathcal{B}(\Lambda_1)$. By Wakimoto [27, Corollary 7.4.6], every connected components of $\mathcal{B}(\Lambda_0) \otimes \mathcal{B}(\Lambda_1)$ is isomorphic to $\mathcal{B}(\Lambda_0 + \Lambda_1)$.

- (ii) If a pair $(\lambda^{(1)}, \lambda^{(2)})$ appears as a vertex of $\mathcal{B}_{2,b}^A$, then both $\lambda^{(1)}$ and $\lambda^{(2)}$ are conjugate distinct-part partitions. However, not every element of the set $\mathcal{P}_{1,b} \times \mathcal{P}_{1,b}$ appears as a vertex of $\mathcal{B}_{2,b}^A$. This follows by comparing the principal specialisation $(-q; q^2)_\infty / (q; q^2)_\infty$ of the character of type $A_1^{(1)}$ and highest weight $\Lambda_0 + \Lambda_1$ with the principal specialisation $(-q; q)_\infty^2$ of the product of the characters of highest weights Λ_0 and Λ_1 .

We represent a grounded partition $\pi \in \mathcal{P}_{2,b}$ as a Young diagram of shape π , with entries a , b or c , as follows. We fill the rightmost cell in each row with the colour (a , b or c) of the corresponding part. Note that all odd columns have an entry a or c at the bottom: the bottom cell of the $(2i + 1)$ th column is assigned the label of the first occurrence of the part $(2i + 1)$ in π . In each column with an odd index, we fill the remaining entries such that the entries along the column alternate between a and c . In each column with an even index, we put an entry b in each cell. This completely determines the entries in the diagram. Given such a diagram, we can recover the grounded partition π by reading the rows from bottom to top to obtain the parts and by reading the last entry in each row to obtain the label of each part. From now on, we identify $\mathcal{P}_{2,b}$ with the set of such diagrams.

We now extend the description of $\mathcal{P}_{2,b}$ as Young diagrams with entries to arbitrary shapes. We place entries in each cell according to the same pattern used for $\mathcal{P}_{2,b}$ and define a colouring of the cells from these entries. This colouring enables us to define the *type* of such a diagram.

Definition 3.6. Let π be a partition, and consider its Young diagram with entries in $\{a, b, c\}$. We give the conditions on the entries, then determine the colour of each cell, and finally define the type of π in terms of both its entries and colours.

- (i) (Entries) All cells in columns with odd indices have entry a or c , while all cells in columns with even indices have entry b . As an initial condition, all cells in the 0th column have entry b .
- (ii) (Colours) For convenience, we call a cell with entry $x \in \{a, b, c\}$ an x -cell. Each cell is coloured either green or blue according to its entry, as follows:
- An a -cell is coloured green, and a c -cell is coloured blue.
 - A b -cell is coloured blue if the cell to its left is an a -cell, and green if the cell to its left is a c -cell.
- (iii) (Type) The *type* of π , denoted $\text{type}(\pi)$, is the binary word defined as follows:
- Read the columns of π from left to right. Assign 0 to a column if its bottom cell is green, and 1 if its bottom cell is blue.
 - If the rightmost cell in the first row is an a -cell, append 00 at the end of the resulting word. If it is a b -cell, append 0.

By the condition that the 0th column consists of b -cells, we have $\text{type}(\emptyset) = 0$. Note that cells along the $(2i + 1)$ th and $(2i + 2)$ th columns have opposite colours. Thus, the colouring is determined by the entries. Conversely, once a colouring of the Young diagram is given, the entries a, b, c of the diagram are uniquely determined by the above conditions.

We now define a directed graph whose vertices are the diagrams with these entries and colouring, and whose structure is determined by their types.

Definition 3.7. The directed graph $\mathcal{B}_{2,b}^P$, with blue and green arrows, is defined recursively starting from the empty partition \emptyset . The vertices are diagrams with entries a, b, c and colouring as in Definition 3.6, obtained inductively during the construction. For each vertex π , the outgoing arrows are determined by the following bracketing rules:

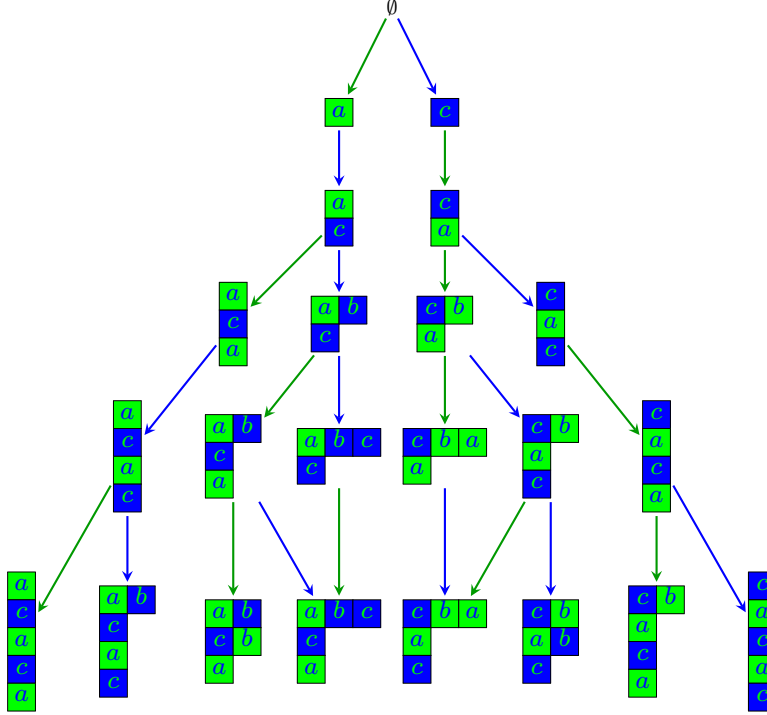
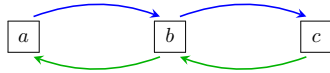


Figure 21: The graph $\mathcal{B}_{2,b}^{\mathcal{P}}$

- (i) **Blue arrow.** Given $\text{type}(\pi)$, assign a left bracket “(” to each letter 0, and a right bracket “)” to each 1. Take the leftmost unmatched 0, and add a blue cell at the bottom of the corresponding column of π . A blue arrow is drawn from π to the resulting diagram.
- (ii) **Green arrow.** Defined in the same way, using the binary word obtained by interchanging the roles of blue and green cells in the definition of $\text{type}(\pi)$; and interchanging the rules of a -cells and c -cells at the end of the first row.

Here, the entry of the newly added cell is determined by Definition 3.6: if the column has odd index, the entry is either a or c , depending on the colour of the cell; if the column has even index, the entry is b . The graph $\mathcal{B}_{2,b}^{\mathcal{P}}$ is shown in Figure 21.

Remark 3.8. The motivation for the definition of the graph $\mathcal{B}_{2,b}^{\mathcal{P}}$ comes from the perfect crystal graph of type $A_1^{(1)}$ at level 2, illustrated as



For the definition and further details on perfect crystal graphs, see [14, Chapter 10]. Perfect crystal graphs, first studied in [16], play an important role in the representation theory of affine Lie algebras. Unlike affine crystal graphs, they have finitely many vertices. An important recursive model for affine crystal graphs, known as the Kyoto path model, is obtained by taking the semi-infinite tensor power of a perfect crystal graph (see [16] or [14, Theorem 10.6.7]).

In Definitions 3.6 and 3.7, the motivation for colouring the cells blue or green comes from the colours of the incoming arrows in the perfect crystal graph: the vertex a only has an incoming green arrow; c only has an incoming blue arrow; the arrow from c to b is green; and the arrow from a to b is blue. Moreover, in the definition of type ,

the motivation for appending additional 0s comes from the perfect crystal: we append two additional 0s at the end of the word if the first row ends with an a -cell because there are two consecutive blue arrows from vertex a in the perfect crystal; we append one additional 0 if the first row ends with a b -cell because there is one blue arrow from vertex b in the perfect crystal.

Remark 3.9. In this remark we explain why the addable-removable corner rule in Definition 1.13 does not generalise from level-1 to level-2 grounded partitions.

- (i) If we defined a graph using addable and removable corners instead of using type, then the grounded partition $\pi = 1_c 2_b 2_b 3_c$ would be the target of two blue arrows, which cannot occur for a crystal graph. Indeed, the grounded partition $1_c 1_a 2_b 3_c$ has three addable blue corners (following the parts 0_b , 1_a and 2_b), and two removable corners (at the ends of the rows 1_c and 3_c). Of the three removable blue corners, one is unmatched, and there is a blue arrow from $1_c 1_a 2_b 3_c$ to π . The grounded partition $1_c 2_b 2_b 2_c$ has one matched and one unmatched removable corner, and there is a blue arrow from $1_c 2_b 2_b 2_c$ to π . In contrast, under Definition 3.7, π has only one incoming blue arrow. This is illustrated in Figure 22.
- (ii) The counterexample in Figure 22 might suggest that we could use the addable–removable corner rule if we make the following extra assumption. Assume that in columns with odd indices, entries a and c alternate. This would resolve the issue in the previous counterexample. However, one can find another counterexample, where the addable–removable corner rule with this extra assumption fails. By observing the asymptotic model (see Definition 3.4), and following the same sequence of arrows for grounded partitions, one can see that there are two consecutive blue arrows starting from the grounded partition $\pi = 1_c 1_a 3_a 3_c 4_b$. Using the addable–removable corner rule with this extra assumption, one of the two addable blue corners in π is matched. In contrast, $\text{type}(\pi) = 10010$ has two unmatched 0s, so there are two consecutive blue arrows starting from π , under Definition 3.7. This is illustrated in Figure 23.

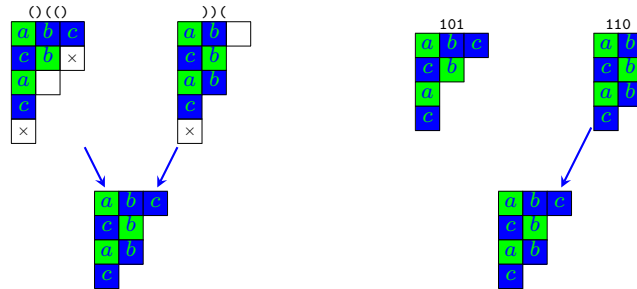


Figure 22: Counterexample for addable–removable corner rule for grounded partitions

Let us make a few observations about the vertices of $\mathcal{B}_{2,b}^{\mathcal{P}}$. From the definition of type and the construction of $\mathcal{B}_{2,b}^{\mathcal{P}}$, it is immediate that one always adds a blue cell below a green cell, and a green cell below a blue cell. Hence, green and blue cells alternate along each column. In particular, columns with odd indices contain entries a and c alternating from bottom to top. Moreover, the colours (blue or green) of cells in a column with even index are determined by the colours of the cells in the adjacent column to the left. It follows that once the colour of any cell in $(2i + 1)$ th or $(2i + 2)$ th columns is given, the colours of all remaining cells in these two columns are uniquely determined.

We can assign a partition, with each part coloured a , b or c , to every vertex of $\mathcal{B}_{2,b}^{\mathcal{P}}$ by reading the rows from bottom to top and assigning to each part the entry of the rightmost cell in the row. In the next proposition, we show that this vertex set coincides with $\mathcal{P}_{2,b}$.

Proposition 3.10. The set of vertices of the graph $\mathcal{B}_{2,b}^{\mathcal{P}}$ is $\mathcal{P}_{2,b}$.

the difference between a consecutive a -part and c -part cannot be 2.

Hence, in the coloured partition assigned to π ,

- the part following $(2k+1)_a$ is $(2k+1)_c$, $(2k+2)_b$, or $(2k+3)_a$,
- the part following $(2k)_b$ is $(2k)_b$, $(2k+1)_a$, or $(2k+1)_c$,
- the part following $(2k+1)_c$ is $(2k+1)_a$, $(2k+2)_b$, or $(2k+3)_c$.

These conditions coincide with the exact difference condition for the matrix M_2 . Hence π is an element of $\mathcal{P}_{2,b}$.

It remains to show that every element $\lambda \in \mathcal{P}_{2,b}$ appears as a vertex of $\mathcal{B}_{2,b}^{\mathcal{P}}$. The proof of the first inclusion shows that arrows map $\mathcal{P}_{2,b}$ into itself.

By Definition 3.7, a vertex π of $\mathcal{B}_{2,b}$ is the target of a green (resp. blue) arrow if and only if there is an unmatched right bracket, where we associate a left bracket “(” to each column of π that has a blue (resp. green) cell at the bottom and a right bracket “)” to each column of π that has a green (resp. blue) cell at the bottom. We extend the definition of inverse arrows to the set $\mathcal{P}_{2,b}$. Assume $\pi \in \mathcal{P}_{2,b}$ is the target of a blue arrow with source μ . We need to show that μ also lies in $\mathcal{P}_{2,b}$. The argument for green arrows is analogous.

- First, we show that the diagram of μ has partition shape, i.e. the columns are weakly decreasing in size. We have seen that there are at most two consecutive columns in π of the same size. If the i th and $(i+1)$ th columns in π have the same size, then the bottom cells are either both blue or both green. Assume they are both blue. Then, if the letter 0 in $\text{type}(\pi)$ corresponding to the i th column is unmatched, so is the letter 0 corresponding to the $(i+1)$ th column, which is further to the left. In other words, the blue cell at the bottom of the i th column of π is still present in μ .
- Next, we show that μ cannot have two consecutive b -parts with difference 2. Assume the i th column of π has a c -cell at the bottom and the size of the $(i+1)$ th column is one less. Then the b -cell at the bottom of the $(i+1)$ th column is also blue, since colours along columns alternate. By the same argument as above, the cell at the bottom of the i th column of π is still present in μ . This is illustrated in the first diagram of Figure 24.
- Assume that both the i th and the $(i+2)$ th columns of π have a c -cell at the bottom; the $(i+1)$ th and the $(i+2)$ th columns have the same size; and the size of the i th column is one greater. Then the b -cell at the bottom of the $(i+1)$ th column is blue. By the same argument as above, the cell at the bottom of the i th column of π is still present in μ . This is illustrated in the second diagram of Figure 24.

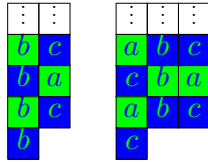


Figure 24: $\mathcal{P}_{2,b}$ is closed for inverse arrows

By definition, 0_b , the unique size-0 element of $\mathcal{P}_{2,b}$, lies in $\mathcal{B}_{2,b}^{\mathcal{P}}$. We proceed by induction on the size of π . Given $\pi \in \mathcal{P}_{2,b}$ of size greater than 0, we need to show that there is either a green or a blue arrow whose target is π .

Assume π is not the target of a green arrow. Then, by definition of the inverse green arrow and because π is nonempty, the bottom cell in the first column is blue. This means, by definition of the inverse blue arrow, that the first bracket in the sequence is a right bracket, which remains unmatched. Thus, π is the target of a blue arrow.

Hence, every element $\pi \in \mathcal{P}_{2,b}$ appears as a vertex of $\mathcal{B}_{2,b}^P$. □

We describe a map δ from the set $\mathcal{P}_{2,b}$ to the set of pairs of partitions. To this end, we decompose the set of cells in the diagram of $\pi \in \mathcal{P}_{2,b}$ into a suitable disjoint union of two sets, S_1 and S_2 . If the first row of π has no a -cells, every cell belongs to S_2 . If there is an a -cell in the first row, consider the horizontal strip starting from the first a -cell in the first row, where each subsequent cell is either an a -cell or a blue b -cell located immediately to the right or immediately below to the right. Repeating this step as long as possible produces a horizontal strip, in which a -cells and blue b -cells alternate. Every cell above and including this strip belongs to S_1 . The remaining cells in π belong to S_2 . This construction is illustrated in Figure 25.

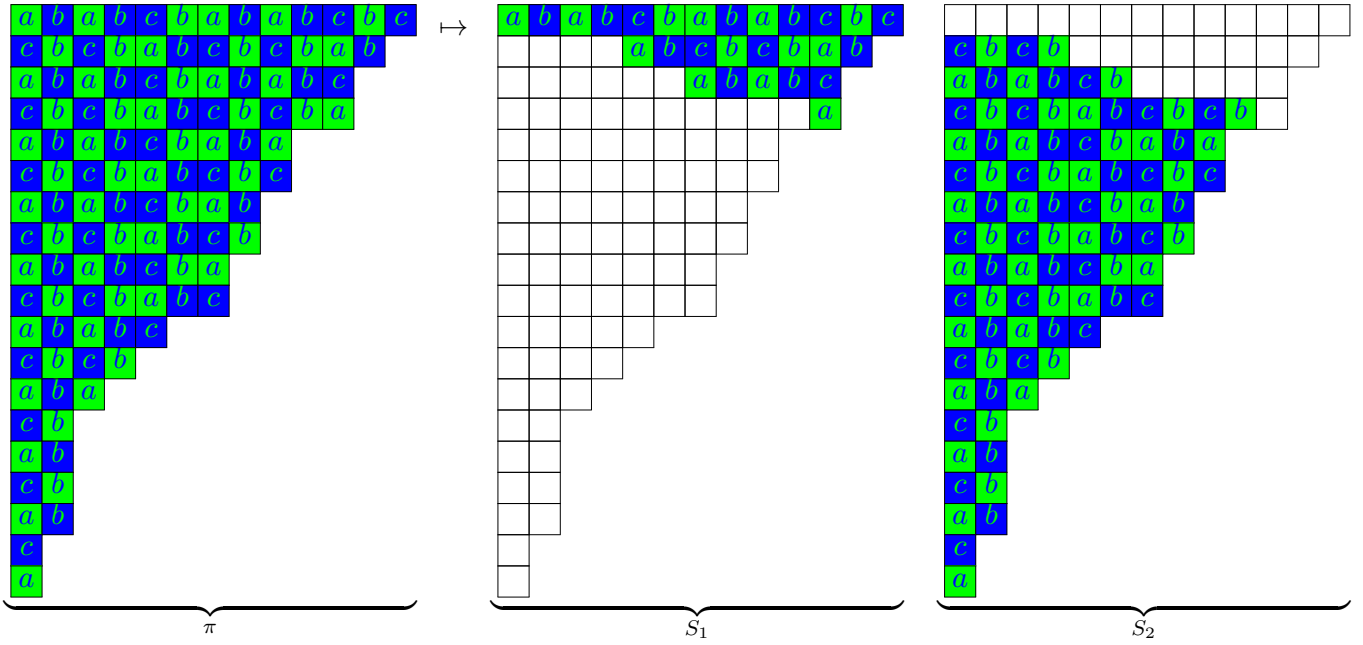


Figure 25: Decomposing π into S_1 and S_2

The partition $\lambda^{(2)}$ is obtained from S_2 by sliding its columns upward and forgetting the entries a, b, c . This is illustrated in Figure 26. In other words, we decompose S_2 into horizontal strips. The horizontal strip along the north wall has alternating c -cells and green b -cells. The next horizontal strip has alternating a -cells and blue b -cells, and so on, with odd-indexed strips having c - and green b -cells alternatingly, and even-indexed strips having a - and blue b -cells alternatingly. Let p_1, p_2, \dots denote the lengths of these horizontal strips. Then $\lambda^{(2)}$ is the partition whose i th part is p_i .

The partition $\lambda^{(1)}$ is constructed from S_1 as follows. We again decompose S_1 into horizontal strips. The horizontal strip along the south wall has alternating a -cells and blue b -cells. The next horizontal strip has alternating c -cells and green b -cells, and so on. Let h_1, h_2, \dots denote the lengths of these horizontal strips. Then $\lambda^{(1)}$ is defined as the partition whose i th column has length h_i . In our example, these horizontal strips have length $(h_1, h_2, h_3, h_4) = (11, 7, 6, 3)$, as illustrated in the middle part of Figure 27. We label the cells of these strips with integers $1, \dots, 4$. Then we have $\lambda^{(1)} = (11, 7, 6, 3)'$.

Lemma 3.11. Let $\pi \in \mathcal{P}_{2,b}$ and $\delta(\pi) = (\lambda^{(1)}, \lambda^{(2)})$. Then $\lambda^{(1)}$ and $\lambda^{(2)}$ are conjugate distinct-part partitions. Moreover, the map δ is injective.

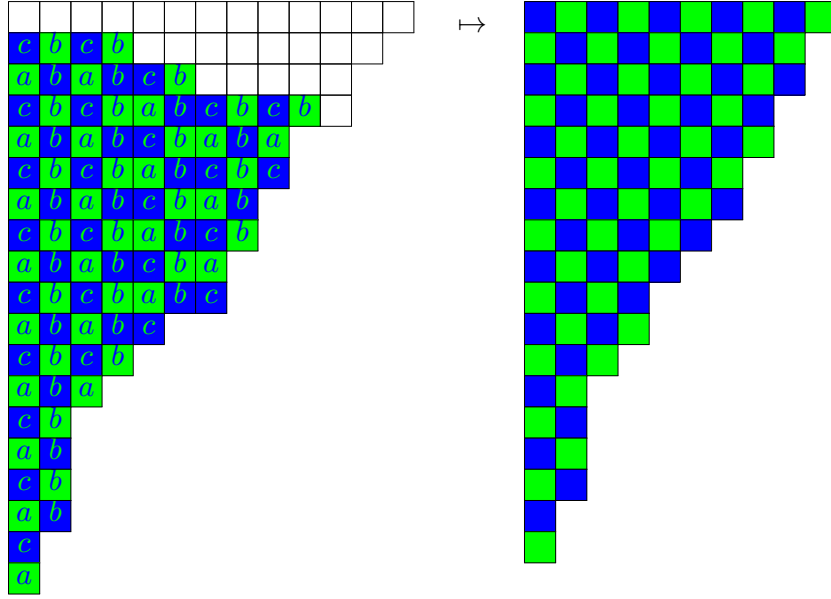


Figure 26: Obtaining $\lambda^{(2)}$ from S_2

Proof. To show that the partition $\lambda^{(1)}$ is a conjugate distinct part partition, consider two consecutive horizontal strips of lengths h_i and h_{i+1} . Note that a horizontal strip contains at most one cell in each column. We compare the sets of columns that contribute cells to these two strips. By construction, there are at least two columns that contribute to h_i but not to h_{i+1} . After these, there may appear columns that contribute simultaneously to both h_i and h_{i+1} , and eventually a column may appear that contributes only to h_{i+1} . However, by the difference conditions of $\mathcal{P}_{2,b}$, there can be at most one such column that contributes to h_{i+1} but not to h_i . Therefore, we conclude that $h_i > h_{i+1}$, and hence, $\lambda^{(1)}$ is a conjugate distinct-part partition.

Now we consider $\lambda^{(2)}$. By the difference conditions of $\mathcal{P}_{2,b}$, there are at most two consecutive columns c_{2i} and c_{2i+1} in π of the same length. We have seen in the proof of Proposition 3.10 that cells in two consecutive columns of the same length have an alternating green-blue domino pattern. By construction, the horizontal strip at the south wall of S_1 does not contain two consecutive cells of the same colour. Thus, if two consecutive columns in π have the same length, then their intersection with S_2 cannot have the same length. In other words, all columns of $\lambda^{(2)}$ are distinct.

Note that the strip at the south wall of S_1 is longer than the strip at the north wall of S_2 if and only if the cell at the top-left corner of π is an a -cell. This follows from the same argument used in the proof that $\lambda^{(1)}$ has distinct columns. Therefore, we can recover the grounded partition π from $\delta(\pi) = (\lambda^{(1)}, \lambda^{(2)})$. Hence, δ is injective. \square

We say that two binary words r and s on the alphabet $\{0, 1\}$ are *equivalent*, written $r \sim s$, if the subwords of r and s restricted to unmatched letters are equal. We then show that δ preserves type up to this equivalence.

Lemma 3.12. We have $\text{type}(\pi) \sim \text{type}(\delta(\pi))$ for all $\pi \in \mathcal{P}_{2,b}$.

Proof. In the description of the map δ , let S_1 and S_2 be the two disjoint unions obtained from the decomposition of the cells of π , as in Figure 25, and let $\delta(\pi) = (\lambda^{(1)}, \lambda^{(2)})$. Let $\text{type}(S_2)$ denote the factor of $\text{type}(\pi)$ consisting of the letters that correspond to bottom cells of columns in S_2 . Note that $\text{type}(\lambda^{(2)}) = \text{type}(S_2)$ if the first row of $\lambda^{(2)}$ ends in blue, and $\text{type}(\lambda^{(2)}) = \text{type}(S_2)0$ if the first row of $\lambda^{(2)}$ ends in green.

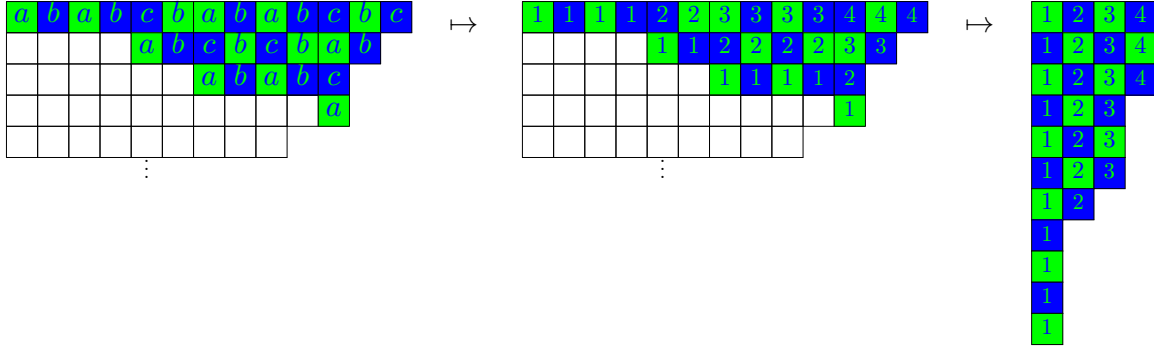


Figure 27: Construction of λ_1 from S_1

Consider the widths of π and S_2 , that is, the numbers of columns containing their cells. Denote these by $w(\pi)$ and $w(S_2)$, respectively. It is clear that $w(\pi) \geq w(S_2)$. We proceed by induction on $w(\pi) - w(S_2)$. For the base case $w(\pi) - w(S_2) = 0$, we distinguish four cases according to the entry and colour of the top and the bottom cell in the last column of π within the region of S_1 . Note that by definition of S_1 , all cells at the south wall of S_1 are either a -cells or blue b -cells, whenever the column continues in S_2 .

- (1a) Assume that the last column of π has an a -cell both at the top and the bottom of S_1 . Since colours alternate along columns and a -cells are green, the first row of $\lambda^{(2)}$ ends in a blue cell. By definition of δ , each strip starts with an a - or c -cell and no strip contains both. Thus, the topmost strip of π starts with an a -cell, and the first row of $\lambda^{(1)}$ ends in green. Since the last column of π intersects S_2 , the strip endings and the cells of the last column within S_1 are in bijection. It follows that

$$\text{type}(\lambda^{(1)}, \lambda^{(2)}) = \text{type}(\lambda^{(2)}) \text{type}(\lambda^{(1)}) = \text{type}(S_2) \cdot 0101 \dots 0100 \sim \text{type}(S_2)00.$$

Since the first row of π ends in an a -cell, we have $\text{type}(\pi) = \text{type}(S_2)00$. Thus, $\text{type}(\pi) \sim \text{type}(\lambda^{(1)}, \lambda^{(2)})$.

- (1b) Assume that the last column of π has a c -cell at the top and an a -cell at the bottom of S_1 . Then, the first row of $\lambda^{(2)}$ ends in a blue cell. Since the topmost strip in π must start with a c -cell, the first row of $\lambda^{(1)}$ ends in blue. Hence

$$\text{type}(\lambda^{(1)}, \lambda^{(2)}) = \text{type}(S_2) \cdot 0101 \dots 01 \sim \text{type}(S_2).$$

As the first row of π ends in a c -cell, we have $\text{type}(\pi) = \text{type}(S_2)$. Therefore, $\text{type}(\pi) \sim \text{type}(\lambda^{(1)}, \lambda^{(2)})$.

- (1c) Assume that the last column of π has a blue b -cell both at the top and the bottom of S_1 . Then, the first row of $\lambda^{(2)}$ ends in a green cell. In any strip that contains a blue b -cell, a -cells and blue b -cells alternate. Hence the topmost strip in π must start with an a -cell, and the first row of $\lambda^{(1)}$ ends in green. It follows that

$$\text{type}(\lambda^{(1)}, \lambda^{(2)}) = \text{type}(S_2)0 \cdot 1010 \dots 1010 \sim \text{type}(S_2)0.$$

Since the first row of π ends in a b -cell, we have $\text{type}(\pi) = \text{type}(S_2)0$. Therefore, $\text{type}(\pi) \sim \text{type}(\lambda^{(1)}, \lambda^{(2)})$.

- (1d) Assume that the last column of π has a green b -cell at the top and a blue b -cell at the bottom of S_1 . Then, the first row of $\lambda^{(2)}$ ends in a green cell. In any strip that contains a green b -cell, c -cells and green b -cells alternate. Hence the topmost strip in π must start with a c -cell, and the first row of $\lambda^{(1)}$ ends in blue. It follows that

$$\text{type}(\lambda^{(1)}, \lambda^{(2)}) = \text{type}(S_2)0 \cdot 1010 \dots 10 \sim \text{type}(S_2)0.$$

Since the first row of π ends in a b -cell, we have $\text{type}(\pi) = \text{type}(S_2)0$. Therefore, $\text{type}(\pi) \sim \text{type}(\lambda^{(1)}, \lambda^{(2)})$.

We now assume that $w(\pi) - w(S_2) > 0$. Let π_\circ denote the grounded partition obtained from π by deleting its last column, and let $\delta(\pi_\circ) = (\lambda_\circ^{(1)}, \lambda_\circ^{(2)})$. By the induction hypothesis, $\text{type}(\pi_\circ) \sim \text{type}(\lambda_\circ^{(1)}, \lambda_\circ^{(2)})$. We need to show that $\text{type}(\pi) \sim \text{type}(\lambda^{(1)}, \lambda^{(2)})$. Let $i + 1$ denote the number of columns of π . We distinguish ten cases according to the entry and colour of the top and bottom cells in the $(i + 1)$ th column, and the top cell in the i th column. For convenience, let T_j and B_j denote the topmost and bottommost cell of the j th column, respectively. For every case, we express $\text{type}(\pi)$ and $\text{type}(\lambda^{(1)}, \lambda^{(2)})$ in terms of $\text{type}(\pi_\circ)$ and $\text{type}(\lambda_\circ^{(1)}, \lambda_\circ^{(2)})$, and then, by the induction hypothesis, show that $\text{type}(\pi) \sim \text{type}(\lambda^{(1)}, \lambda^{(2)})$.

- (2a) Assume that T_i, T_{i+1} , and B_{i+1} are a green b -cell, an a -cell, and an a -cell, respectively, illustrated in Figure 28. Then the cell to the left of B_{i+1} is a green b -cell. We have

$$\text{type}(\pi_\circ) = s0, \quad \text{and} \quad \text{type}(\pi) = s000,$$

for some binary word s .

An even number of strips descend one row lower from the i th column to the $(i + 1)$ th column; and a new strip starts in the top cell of the $(i + 1)$ th column, which is a green cell. All strips continuing from π_\circ to π change the colour of the strip ending cell from green to blue, or from blue to green. All other strip endings in π_\circ are unchanged in π . Note that the topmost strip in π starts with an a -cell, so the first row of $\lambda^{(1)}$ ends in green; the topmost strip in π_\circ starts with a c -cell, so the first row of $\lambda_\circ^{(1)}$ ends in blue. Moreover, if the green b -cell to the left of B_{i+1} belongs to S_1 , then the topmost strip ending that remains unchanged is green. If this green b -cell belongs to S_2 , then all strip endings in π_\circ are changed and the last letter of $\text{type}(\lambda^{(2)})$ is 0. These two cases are illustrated by the last two diagrams in Figure 28. Therefore,

$$\text{type}(\lambda_\circ^{(1)}, \lambda_\circ^{(2)}) = r01010\dots10 \sim r0, \quad \text{and} \quad \text{type}(\lambda^{(1)}, \lambda^{(2)}) = r00101\dots0100 \sim r000,$$

for some binary word r .

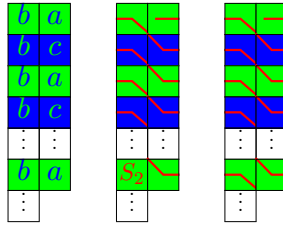


Figure 28: Inductive step, case (2a)

- (2b) Assume that T_i, T_{i+1} , and B_{i+1} are a blue b -cell, a c -cell, and a c -cell, respectively, illustrated in Figure 29. Then the cell to the left of B_{i+1} is a blue b -cell. We have

$$\text{type}(\pi_\circ) = s0, \quad \text{and} \quad \text{type}(\pi) = s1,$$

for some binary word s .

An even number of strips descend one row lower from the i th column to the $(i + 1)$ th column; and a new strip starts in the top cell of the $(i + 1)$ th column, which is a blue cell. All other strip endings in π_\circ are unchanged. Note that the topmost strip in π starts with an c -cell, so the first row of $\lambda^{(1)}$ ends in blue; the topmost strip in π_\circ starts with a a -cell, so the first row of $\lambda_\circ^{(1)}$ ends in green. Therefore,

$$\text{type}(\lambda_\circ^{(1)}, \lambda_\circ^{(2)}) = r0101\dots010 \sim r0, \quad \text{and} \quad \text{type}(\lambda^{(1)}, \lambda^{(2)}) = r1010\dots101 \sim r1,$$

for some binary word r .

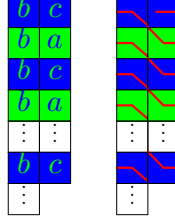


Figure 29: Inductive step, case (2b)

- (2c) Assume that T_i , T_{i+1} , and B_{i+1} are a green b -cell, an a -cell, and a c -cell, respectively, illustrated in Figure 30. Then the cell to the left of B_{i+1} is a blue b -cell. We have

$$\text{type}(\pi_\circ) = s0, \quad \text{and} \quad \text{type}(\pi) = s100,$$

for some binary word s .

An odd number of strips descend one row lower from the i th column to the $(i+1)$ th column; and a new strip starts in the top cell of the $(i+1)$ th column, which is a green cell. All other strip endings in π_\circ are unchanged. Note that the topmost strip in π starts with an a -cell, so the first row of $\lambda^{(1)}$ ends in green; the topmost strip in π_\circ starts with a c -cell, so the first row of $\lambda_\circ^{(1)}$ ends in blue. Therefore,

$$\text{type}(\lambda_\circ^{(1)}, \lambda_\circ^{(2)}) = r0101\dots010 \sim r0, \quad \text{and} \quad \text{type}(\lambda^{(1)}, \lambda^{(2)}) = r1010\dots10100 \sim r100,$$

for some binary word r .

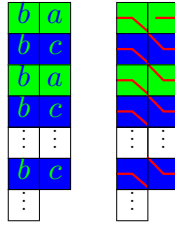


Figure 30: Inductive step, case (2c)

- (2d) Assume that T_i , T_{i+1} , and B_{i+1} are a blue b -cell, a c -cell, and an a -cell, respectively, illustrated in Figure 31. Then the cell to the left of B_{i+1} is a green b -cell. We have

$$\text{type}(\pi_\circ) = s0, \quad \text{and} \quad \text{type}(\pi) = s0,$$

for some binary word s .

An odd number of strips descend one row lower from the i th column to the $(i+1)$ th column; and a new strip starts in the top cell of the $(i+1)$ th column, which is a blue cell. All other strip endings in π_\circ are unchanged. Note that the topmost strip in π starts with a c -cell, so the first row of $\lambda^{(1)}$ ends in blue; the topmost strip in π_\circ starts with an a -cell, so the first row of $\lambda_\circ^{(1)}$ ends in green. Moreover, if the green b cell to the left of B_{i+1} belongs to S_1 , then the topmost strip ending that remains unchanged is green. If this green b -cell belongs to S_2 , then all strip endings in π_\circ are changed and the last letter of $\text{type}(\lambda^{(2)})$ is 0. These two cases are illustrated by the last two diagrams in Figure 31. Therefore,

$$\text{type}(\lambda_\circ^{(1)}, \lambda_\circ^{(2)}) = r01010\dots1010 \sim r0, \quad \text{and} \quad \text{type}(\lambda^{(1)}, \lambda^{(2)}) = r00101\dots0101 \sim r0,$$

for some binary word r .

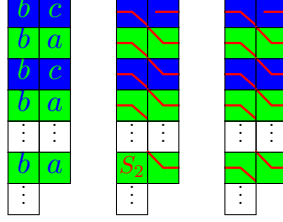


Figure 31: Inductive step, case (2d)

- (2e) Assume that T_i and B_{i+1} are c -cells and a blue b -cell, respectively, illustrated in Figure 32. Then T_{i+1} is a green b -cell, and the cell to the left of B_{i+1} is an a -cell. We have

$$\text{type}(\pi_\circ) = s, \quad \text{and} \quad \text{type}(\pi) = s10,$$

for some binary word s .

An even number of strips traverse the i th and the $(i+1)$ th column horizontally. All other strip endings in π_\circ are unchanged. Note that the topmost strip in both π and π_\circ starts with a c -cell, so the first row of both $\lambda^{(1)}$ and $\lambda_\circ^{(1)}$ ends in blue. Therefore,

$$\text{type}(\lambda_\circ^{(1)}, \lambda_\circ^{(2)}) = r0101\dots01 \sim r, \quad \text{and} \quad \text{type}(\lambda^{(1)}, \lambda^{(2)}) = r1010\dots10 \sim r10,$$

for some binary word r .

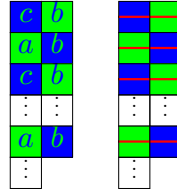


Figure 32: Inductive step, case (2e)

- (2f) Assume that T_i , T_{i+1} , and B_{i+1} are a green b -cell, a c -cell, and a c -cell, respectively, illustrated in Figure 33. Then the cell to the left of B_{i+1} is a green b -cell. We have

$$\text{type}(\pi_\circ) = s0, \quad \text{and} \quad \text{type}(\pi) = s1,$$

for some binary word s .

An odd number of strips traverse the i th and the $(i+1)$ th column horizontally. All other strip endings in π_\circ are unchanged. Note that the topmost strip in both π and π_\circ starts with a c -cell, so the first row of both $\lambda^{(1)}$ and $\lambda_\circ^{(1)}$ ends in blue. Therefore,

$$\text{type}(\lambda_\circ^{(1)}, \lambda_\circ^{(2)}) = r0101\dots010 \sim r0, \quad \text{and} \quad \text{type}(\lambda^{(1)}, \lambda^{(2)}) = r1010\dots101 \sim r1$$

for some binary word r .

- (2g) Assume that T_i , T_{i+1} , and B_{i+1} are a green b -cell, a c -cell, and an a -cell, respectively, illustrated in Figure 34. Then the b -cell to the left of B_{i+1} is blue. We have

$$\text{type}(\pi_\circ) = s0, \quad \text{and} \quad \text{type}(\pi) = s0,$$

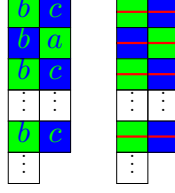


Figure 33: Inductive step, case (2f)

for some binary word s .

An even number of strips traverse the i th and the $(i + 1)$ th column horizontally. All other strip endings in π_\circ are unchanged. Note that the topmost strip in both π and π_\circ starts with a c -cell, so the first row of both $\lambda^{(1)}$ and $\lambda_\circ^{(1)}$ ends in blue. Since T_i is a green b -cell, the cells in the $(i - 1)$ th column are the same as those in the $(i + 1)$ th column in each row. Thus, by the difference conditions of $\mathcal{P}_{2,b}$, the i th and $(i + 1)$ th columns cannot have the same length (see the first diagram in Figure 34). Therefore, there is a green b cell in the i th column, diagonally south-west of B_{i+1} . If this green b -cell belongs to S_1 , then the topmost strip ending of π_\circ that remains unchanged contributes a letter 0. If this green b -cell belongs to S_2 , then all strip endings in π_\circ are changed and the last letter of $\text{type}(\lambda^{(2)})$ is 0. These two cases are illustrated by the last two diagrams in Figure 34. Therefore,

$$\text{type}(\lambda_\circ^{(1)}, \lambda_\circ^{(2)}) = r 0 1010 10 \sim r0, \quad \text{and} \quad \text{type}(\lambda^{(1)}, \lambda^{(2)}) = r 0 0101 \dots 01 \sim r0,$$

for some binary word r .

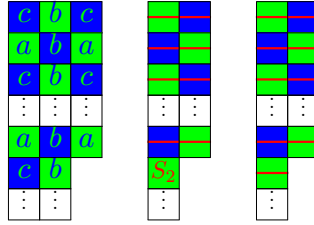


Figure 34: Inductive step, case (2g)

- (2h) Assume that T_i and B_{i+1} are an a -cell and a green b -cell, respectively, illustrated in Figure 35. Then T_{i+1} is a blue b -cell, and the cell to the left of B_{i+1} is a c -cell. We have

$$\text{type}(\pi_\circ) = s00, \quad \text{and} \quad \text{type}(\pi) = s00,$$

for some binary word s .

An even number of strips traverse the i th and the $(i + 1)$ th column horizontally. All other strip endings in π_\circ are unchanged. Note that the topmost strip in both π and π_\circ starts with an a -cell, so the first row of both $\lambda^{(1)}$ and $\lambda_\circ^{(1)}$ ends in green. By the difference conditions in $\mathcal{P}_{2,b}$, there must be an a -cell diagonally south-west of the b -cell B_{i+1} . Moreover, by definition of the map δ , this cell must belong to S_1 . Thus, the topmost strip ending of π_\circ that remains unchanged contributes a letter 0. Therefore,

$$\text{type}(\lambda_\circ^{(1)}, \lambda_\circ^{(2)}) = r 0 1010 \dots 100 \sim r00, \quad \text{and} \quad \text{type}(\lambda^{(1)}, \lambda^{(2)}) = r 0 0101 \dots 010 \sim r00,$$

for some binary word r .

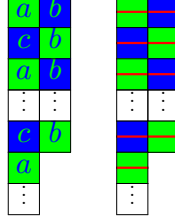


Figure 35: Inductive step, case (2h)

- (2i) Assume that T_i , T_{i+1} , and B_{i+1} are a blue b -cell, an a -cell, and a c -cell, respectively, illustrated in Figure 36. Then the cell to the left of B_{i+1} is a green b -cell. We have

$$\text{type}(\pi_\circ) = s0, \quad \text{and} \quad \text{type}(\pi) = s100,$$

for some binary word s .

An even number of strips traverse the i th and the $(i+1)$ th column horizontally. All other strip endings in π_\circ are unchanged. Note that the topmost strip in both π and π_\circ starts with a a -cell, so the first row of both $\lambda^{(1)}$ and $\lambda_\circ^{(1)}$ ends in green. Therefore,

$$\text{type}(\lambda_\circ^{(1)}, \lambda_\circ^{(2)}) = r0101\dots010 \sim r0, \quad \text{and} \quad \text{type}(\lambda^{(1)}, \lambda^{(2)}) = r1010\dots100 \sim r100,$$

for some binary word r .

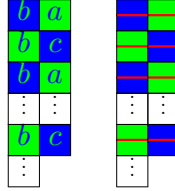


Figure 36: Inductive step, case (2i)

- (2j) Assume that T_i , T_{i+1} , and B_{i+1} are a blue b -cell, an a -cell, and an a -cell, respectively, illustrated in Figure 37. Then the cell to the left of B_{i+1} is a blue b -cell. We have

$$\text{type}(\pi_\circ) = s0, \quad \text{and} \quad \text{type}(\pi) = s000,$$

for some binary word s .

An odd number of strips traverse the i th and the $(i+1)$ th column horizontally. All other strip endings in π_\circ are unchanged. Note that the topmost strip in both π and π_\circ starts with an a -cell, so the first row of both $\lambda^{(1)}$ and $\lambda_\circ^{(1)}$ ends in green. Since T_i is a blue b -cell, the cells in the $(i-1)$ th column are the same as those in the $(i+1)$ th column in each row. Thus, by the difference conditions of $\mathcal{P}_{2,b}$, the i th and $(i+1)$ th columns cannot have the same length (see the first diagram in Figure 37). Therefore, there is a green b -cell in the i th column, diagonally south-west of B_{i+1} . If this green b -cell belongs to S_1 , then the topmost strip ending of π_\circ that remains unchanged contributes a letter 0. If this green b -cell belongs to S_2 , then all strip endings in π_\circ are changed and the last letter of $\text{type}(\lambda^{(2)})$ is 0. These two cases are illustrated by the last two diagrams in Figure 37. Therefore,

$$\text{type}(\lambda_\circ^{(1)}, \lambda_\circ^{(2)}) = r0101\dots1010 \sim r0, \quad \text{and} \quad \text{type}(\lambda^{(1)}, \lambda^{(2)}) = r00101\dots0100 \sim r000,$$

for some binary word r .

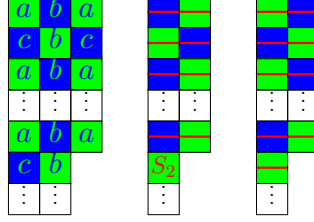


Figure 37: Inductive step, case (2j)

□

We now have all the ingredients to show that δ is a graph isomorphism.

Theorem 3.13. The graphs $\mathcal{B}_{2,b}^{\mathcal{P}}$ and $\mathcal{B}_{2,b}^{\mathcal{A}}$ are isomorphic under the map δ .

Proof. By Proposition 3.10, the vertex set of $\mathcal{B}_{2,b}^{\mathcal{P}}$ is $\mathcal{P}_{2,b}$, and, by Lemma 3.11, the map δ is injective. To prove that δ is a graph isomorphism, it suffices to show the following two conditions:

- (i) $v \in \mathcal{P}_{2,b}$ if and only if $\delta(v)$ is a vertex of $\mathcal{B}_{2,b}^{\mathcal{A}}$, and
- (ii) there is a blue (resp. green) arrow $v \rightarrow w$ in $\mathcal{B}_{2,b}^{\mathcal{P}}$ if and only if there is a blue (resp. green) arrow $\delta(v) \rightarrow \delta(w)$ in $\mathcal{B}_{2,b}^{\mathcal{A}}$.

We prove this by induction on the size. Here, the size of a pair of partitions is defined as the sum of the sizes of the two partitions. For the base case $n = 0$, the claim is immediate since $\delta(\emptyset) = (\emptyset, \emptyset)$. Assume that for all grounded partitions v of size at most n , the map δ satisfies conditions (i) and (ii). This implies the surjectivity of δ on elements of size n , that is, a vertex of $\mathcal{B}_{2,b}^{\mathcal{A}}$ of size n can be written as $\delta(v)$ for some $v \in \mathcal{P}_{2,b}$ of size n .

Suppose there is a blue arrow $v \rightarrow w$ in $\mathcal{B}_{2,b}^{\mathcal{P}}$, and a blue arrow $\delta(v) \rightarrow (\lambda^{(1)}, \lambda^{(2)})$ in $\mathcal{B}_{2,b}^{\mathcal{A}}$ (the same argument applies for a green arrow). By Lemma 3.12, the types of v and $\delta(v)$ are equivalent. Since w and $(\lambda^{(1)}, \lambda^{(2)})$ both arise from the equivalent elements v and $\delta(v)$, and in each case the transformation of the type is obtained by changing the leftmost unmatched 0 into a 1, it follows that w and $(\lambda^{(1)}, \lambda^{(2)})$ are also equivalent. Therefore,

$$\text{type}(\delta(w)) \sim \text{type}(w) \sim \text{type}(\lambda^{(1)}, \lambda^{(2)}).$$

Since both $\delta(w)$ and $(\lambda^{(1)}, \lambda^{(2)})$ are obtained from $\delta(v)$ by adding a single cell, and they are equivalent, we conclude that $\delta(w) = (\lambda^{(1)}, \lambda^{(2)})$.

Every vertex of $\mathcal{B}_{2,b}^{\mathcal{A}}$ with size $n + 1$ arises from the vertices of $\mathcal{B}_{2,b}^{\mathcal{A}}$ with size n in this way. Therefore, for every vertex w of size $n + 1$, we have $w \in \mathcal{B}_{2,b}^{\mathcal{P}}$ if and only if $\delta(w) \in \mathcal{B}_{2,b}^{\mathcal{A}}$, and a blue arrow $v \rightarrow w$ in $\mathcal{B}_{2,b}^{\mathcal{P}}$ if and only if $\delta(v) \rightarrow \delta(w)$ in $\mathcal{B}_{2,b}^{\mathcal{A}}$. Hence conditions (i) and (ii) hold for all partitions of size at most $n + 1$, which completes the proof. □

Remark 3.14. The representation-theoretic interpretation of Lemma 3.12 is that the map δ intertwines with the operators ε_i and φ_i (see [14, equation (4.9)]), and Theorem 3.13 states that δ is a crystal isomorphism (see [14, Definition 4.2.9]).

As a direct consequence of Theorem 3.13, we have the main result of this section.

Theorem 3.15. The graph $\mathcal{B}_{2,b}^{\mathcal{P}}$ is the affine crystal graph of highest weight $\Lambda_0 + \Lambda_1$ and type $A_1^{(1)}$.

In addition to the affine crystal graph of highest weight $\Lambda_0 + \Lambda_1$, in the remaining part of this section we provide grounded partition models for the affine crystal graphs of type $A_1^{(1)}$ and highest weight $2\Lambda_0$ and $2\Lambda_1$. To obtain these, it suffices to interchange the roles of columns with even indices (including the 0th column) and columns with odd indices.

Definition 3.16. The directed graph $\mathcal{B}_{2,ac}^{\mathcal{P}}$ (resp. $\mathcal{B}_{2,ca}^{\mathcal{P}}$) is defined in the same way as Definition 3.7, where the entries, colours, and types of diagrams are defined as in Definition 3.6, except the condition on the entries:

- (i') All cells in columns with even indices have entry a or c , while all cells in columns with odd indices have entry b . As an initial condition, the cells in the 0th column from top to bottom are a, c, a, c, \dots (resp. c, a, c, a, \dots).

The graph $\mathcal{B}_{2,ac}^{\mathcal{P}}$ is shown in Figure 38. By the same argument as the proof of Proposition 3.10, we can explicitly characterise the vertices of $\mathcal{B}_{2,ac}^{\mathcal{P}}$ and $\mathcal{B}_{2,ca}^{\mathcal{P}}$. The vertex sets $\mathcal{P}_{2,ac}$ and $\mathcal{P}_{2,ca}$ of the graphs $\mathcal{B}_{2,ac}^{\mathcal{P}}$ and $\mathcal{B}_{2,ca}^{\mathcal{P}}$ are given by

$$\mathcal{P}_{2,ac} = \{\pi \in \mathcal{P}_{2,a} \mid \ell(\pi) \text{ is even}\} \sqcup \{\pi \in \mathcal{P}_{2,c} \mid \ell(\pi) \text{ is odd}\},$$

and

$$\mathcal{P}_{2,ca} = \{\pi \in \mathcal{P}_{2,c} \mid \ell(\pi) \text{ is even}\} \sqcup \{\pi \in \mathcal{P}_{2,a} \mid \ell(\pi) \text{ is odd}\},$$

respectively.

Remark 3.17. Similarly to Remark 1.8, there is a simple size-preserving bijection between $\mathcal{P}_{2,a}$ (resp. $\mathcal{P}_{2,c}$) and $\mathcal{P}_{2,ac}$ (resp. $\mathcal{P}_{2,ca}$), given by swapping the colours a and c when the length is odd; and by the identity when the length is even. However, for the graph isomorphism, it is essential to have alternating entries a and c in the 0th column.

The asymptotic model $\mathcal{B}_{2,ac}^A$ (resp. $\mathcal{B}_{2,ca}^A$) of highest weight $2\Lambda_1$ (resp. $2\Lambda_0$) is defined in the same way as $\mathcal{B}_{2,b}^A$, except that both partitions $\lambda^{(1)}$ and $\lambda^{(2)}$ have a green (resp. blue) cell in the top-left corner. The graph $\mathcal{B}_{2,ac}^A$ is illustrated in Figure 39. The graph $\mathcal{B}_{2,ca}^A$ is obtained from $\mathcal{B}_{2,ac}^A$ by interchanging green and blue cells as well as green and blue arrows.

In defining δ , we follow the same idea: cells in the first row contribute to S_2 as long as the colours blue and green alternate. Once a colour repeats, all remaining cells in the first row contribute to S_1 , and the alternating-colour horizontal strip continues in the next row. This process is repeated until reaching the edge of the partition. Every cell below and including this horizontal strip contributes to S_2 , and every cell above it contributes to S_1 . The construction of $\lambda^{(1)}$ and $\lambda^{(2)}$ from S_1 and S_2 is analogous to that of $\mathcal{B}_{2,b}^{\mathcal{P}}$.

If π is a vertex of $\mathcal{B}_{2,ac}^{\mathcal{P}}$, then in the first horizontal strip contributing to S_2 , the c -cells and green b -cells alternate. This is illustrated in Figure 40. Similarly, if π is a vertex of $\mathcal{B}_{2,ca}^{\mathcal{P}}$, then in the first horizontal strip contributing to S_2 , the a -cells and blue b -cells alternate.

Analogously to the proof of Theorem 3.13, it follows that δ is again a graph isomorphism in both cases. As a direct consequence of this, we have the following result.

Theorem 3.18. The graph $\mathcal{B}_{2,ac}^{\mathcal{P}}$ (resp. $\mathcal{B}_{2,ca}^{\mathcal{P}}$) is the affine crystal graph of highest weight $2\Lambda_1$ (resp. $2\Lambda_0$) and type $A_1^{(1)}$.

4 Decomposition formulas at levels 1 and 2

We consider the following question on affine crystal graphs at levels 1 and 2 of type $A_1^{(1)}$: what happens when the green (affine) arrows are erased from the affine crystal graphs in Definitions 1.14 and 3.7? This corresponds to a

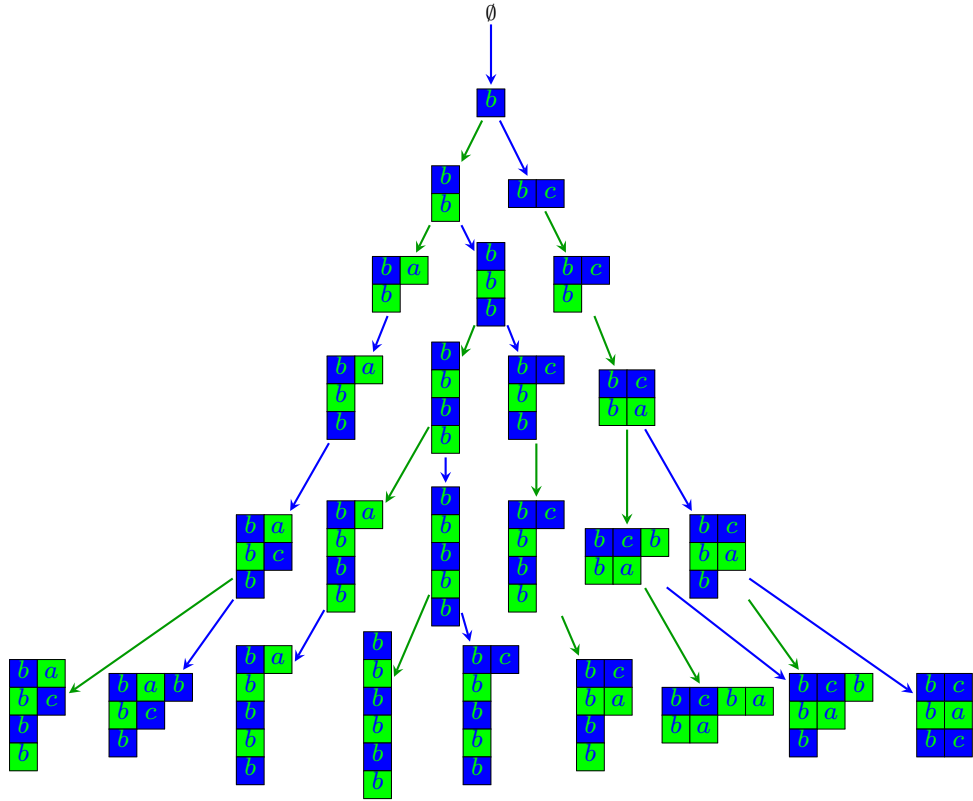


Figure 38: The graph $\mathcal{B}_{2,ac}^P$

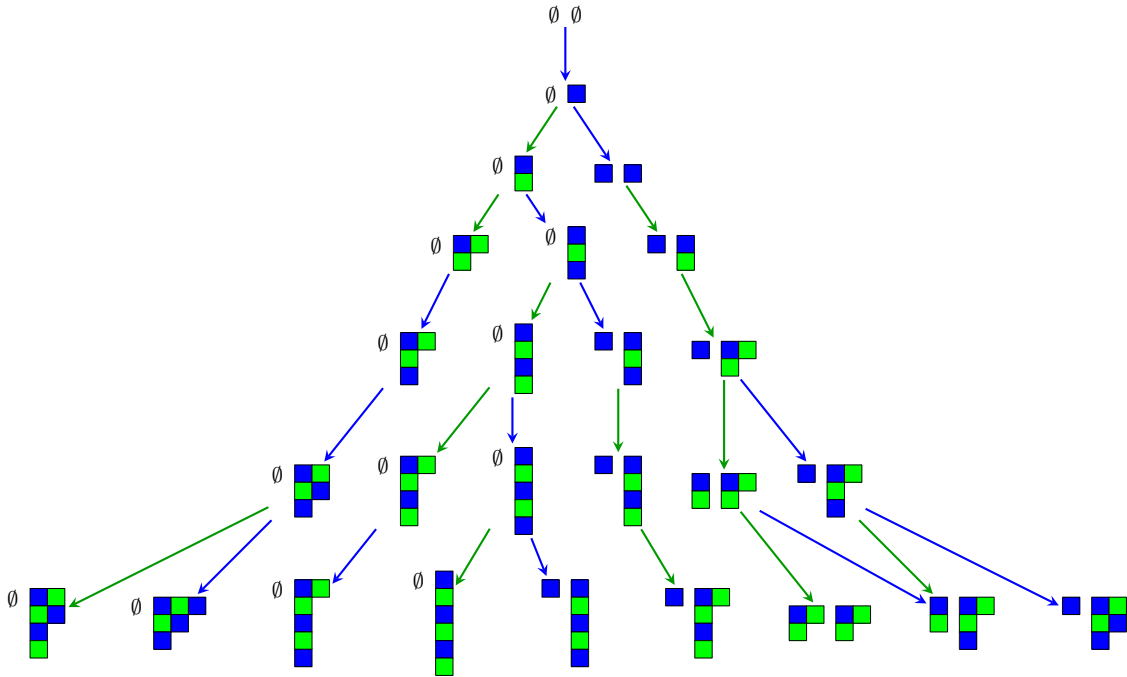


Figure 39: The graph $\mathcal{B}_{2,ac}^A$

(iii) The *q-binomial coefficient* is defined, for all $n \geq k \geq 0$, as

$$\begin{bmatrix} n \\ k \end{bmatrix}_q := \frac{[n]_q!}{[k]_q! [n-k]_q!}.$$

Example 4.3. (i) The generating function of the major index on the symmetric group S_n is

$$\sum_{\pi \in S_n} q^{\text{maj } \pi} = [n]_q!.$$

(ii) Let $\mathcal{L}(n, k)$ denote the set of binary words with n many 0s and k many 1s. The generating function of major index on $\mathcal{L}(n, k)$ is

$$\sum_{\pi \in \mathcal{L}(n, k)} q^{\text{maj } \pi} = \begin{bmatrix} n+k \\ k \end{bmatrix}_q.$$

Remark 4.4. In Subsection 4.3, we need the fact that *q*-binomial coefficients are *palindromic*, i.e. the coefficients are symmetric in the middle. This can be seen as follows. Given a word w on the alphabet of nonnegative integers, a *inversion* is a pair (i, j) where $i < j$ and $w_i > w_j$. The generating function of inversions and major index coincides both on permutations and binary words (see Stanley [26, Proposition 1.4.6]). The palindromicity of *q*-binomial coefficients can be seen from the inversion interpretation of *q*-binomials (see Stanley [26, Proposition 1.7.3]).

Definition 4.5. A word on the alphabet $\{0, 1\}$ is called a *Yamanouchi word* if the number of 0s is at least as large as the number of 1s in each prefix. We denote the set of Yamanouchi words with n many 0s and k many 1s by $\mathcal{Y}(n, k)$. A Yamanouchi word $w \in \mathcal{Y}(n, k)$ with $n = k$ is called a *Dyck word*.

Example 4.6. A *Dyck path* of length $2n$ is a lattice path from $(0, 0)$ to (n, n) consisting of up steps $(0, 1)$ and right steps $(1, 0)$ that stays weakly above the main diagonal. We can identify Dyck words in $\mathcal{Y}(n, n)$ with Dyck paths of length $2n$, where each letter 0 corresponds to an up step and each letter 1 to a right step. In Figure 41, we list all 14 Dyck words of length 8 together with the corresponding Dyck paths. It is well-known (see [2, Theorem 10.3.1])

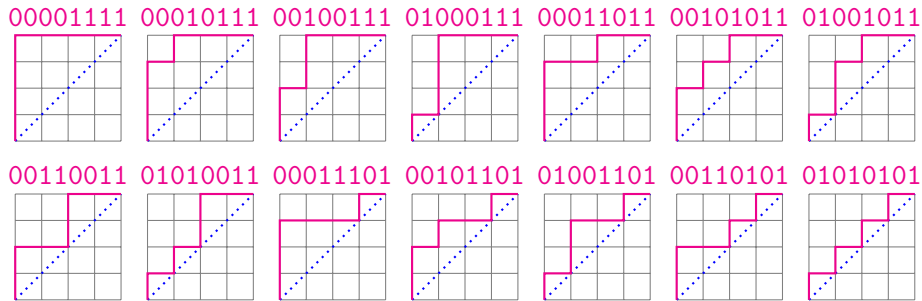


Figure 41: Dyck words of length 8 together with the corresponding Dyck paths

that the number of Dyck paths of length $2n$ is the n th Catalan number:

$$\frac{1}{n+1} \binom{2n}{n}.$$

The major index on Dyck words of length 8 is given by

$$\begin{array}{ccccccc} \overset{0}{00001111}, & \overset{4}{00010111}, & \overset{3}{00100111}, & \overset{2}{01000111}, & \overset{5}{00011011}, & \overset{5+3}{00101011}, & \overset{5+2}{01001011}, \\ \overset{4}{00110011}, & \overset{4+2}{01010011}, & \overset{6}{00011101}, & \overset{6+3}{00101101}, & \overset{6+2}{01001101}, & \overset{6+4}{00110101}, & \overset{6+4+2}{01010101}. \end{array}$$

and the generating function of the major index is again a q -analogue of the number of words:

$$1 + q^2 + q^3 + 2q^4 + q^5 + 2q^6 + q^7 + 2q^8 + q^9 + q^{10} + q^{12} = \frac{1}{[4+1]_q} \begin{bmatrix} 8 \\ 4 \end{bmatrix}_q.$$

In general, the generating function of $\text{maj}(w)$ on Dyck words of length $2n$ is given by

$$\sum_{w \in \mathcal{Y}(n,n)} q^{\text{maj}(w)} = \frac{1}{[n+1]_q} \begin{bmatrix} 2n \\ n \end{bmatrix}_q. \quad (4.1)$$

This theorem is due to MacMahon [22], and a bijective proof was given by F\"urlinger and Hofbauer in [11].

The number of Yamanouchi words in $\mathcal{Y}(n, k)$ is

$$\frac{n-k+1}{n+1} \binom{n+k}{n}.$$

This classical result appears in [2, Corollary 10.3.2]. We now define a q -analogue of this binomial expression, which was first considered by Carlitz and Riordan [4].

Definition 4.7. The q -Yamanouchi number $Y_q(n, k)$ is defined as

$$Y_q(n, k) := \frac{[n-k+1]_q}{[n+1]_q} \begin{bmatrix} n+k \\ n \end{bmatrix}_q.$$

However, the generating function of the major index on Yamanouchi words is not the q -analogue $Y_q(n, k)$. In fact, the coefficients of the generating function of the major index on $\mathcal{Y}(n, k)$ are not even palindromic, unlike those of the q -Yamanouchi numbers (indeed, we have seen in Remark 4.4 that the q -binomial coefficients are palindromic).

Definition 4.8. For a finite binary word w , append an additional letter 0 at the end of w . Then the *modified major index* $\widetilde{\text{maj}}(w)$ of w is defined as the major index of this new word with the dummy 0. In other words, whenever w ends with a letter 1, we add its length to its major index; otherwise the major index remains unchanged.

Example 4.9. The modified major index statistic on $\mathcal{Y}(5, 3)$ is as follows.

$$\begin{array}{ccccccc} 8 & 8+5 & 8+4 & 8+3 & 8+2 & 8+6 & 8+6+4 \\ 000001110, & 000010110, & 000100110, & 001000110, & 010000110, & 000011010, & 000101010, \\ 8+6+3 & 8+6+2 & 8+8+5 & 8+5+3 & 8+5+2 & 8+4 & 8+4+2 \\ 001001010, & 010001010, & 000110010, & 001010010, & 010010010, & 001100010, & 010100010, \\ 7 & 7+4 & 7+3 & 7+2 & 7+5 & 7+5+3 & 7+5+2 \\ 000011100, & 000101100, & 001001100, & 010001100, & 000110100, & 001010100, & 010010100, \\ 7+4 & 7+4+2 & 6 & 6+3 & 6+2 & 6+4 & 6+4+2 \\ 001100100, & 010100100, & 000111000, & 001011000, & 010011000, & 001101000, & 010101000. \end{array}$$

The generating function is the q -analogue $Y_q(n, k)$, multiplied with the factor q^6 :

$$\sum_{w \in \mathcal{Y}(5,3)} q^{\widetilde{\text{maj}}(w)} = q^6 + q^7 + 2q^8 + 2q^9 + 3q^{10} + 3q^{11} + 4q^{12} + 3q^{13} + 3q^{14} + 2q^{15} + 2q^{16} + q^{17} + q^{18} = q^6 \frac{[3]_q}{[6]_q} \begin{bmatrix} 8 \\ 3 \end{bmatrix}_q.$$

Proposition 4.10. We have

$$\sum_{w \in \mathcal{Y}(n,k)} q^{\widetilde{\text{maj}}(w)} = q^{2k} Y_q(n, k) \quad (4.2)$$

This result is essentially a special case of [18, Theorem 5]. Since we use a slightly different modification of the major index, we include a proof for completeness.

Lemma 4.11. Let $\mathcal{L}(n, k)$ denote the set of all binary words with n many 0s and k many 1s. For any $n, k \in \mathbb{N}$, we have

$$\sum_{w \in \mathcal{L}(n, k)} q^{\widetilde{\text{maj}}(w)} = q^k \begin{bmatrix} n+k \\ k \end{bmatrix}_q. \quad (4.3)$$

Proof. We proceed by induction on the length $n+k$. In the base case $n = k = 0$, both sides are equal to 1. Assume the statement holds for all lengths less than $n+k$.

Let $\mathcal{L}_0(n, k)$ be the subset of $\mathcal{L}(n, k)$ consisting of words that end with 0, and let $\mathcal{L}_1(n, k)$ be the subset consisting of words that end with 1. By the induction hypothesis, we have

$$\sum_{w \in \mathcal{L}_0(n, k)} q^{\widetilde{\text{maj}}(w)} = \sum_{w \in \mathcal{L}(n-1, k)} q^{\widetilde{\text{maj}}(w)} = q^k \begin{bmatrix} n+k-1 \\ k \end{bmatrix}_q. \quad (4.4)$$

By the basic fact in Example 4.3 (ii), we have

$$\sum_{w \in \mathcal{L}_1(n, k)} q^{\widetilde{\text{maj}}(w)} = \sum_{w \in \mathcal{L}(n, k-1)} q^{n+k+\text{maj}(w)} = q^{n+k} \begin{bmatrix} n+k-1 \\ k-1 \end{bmatrix}_q. \quad (4.5)$$

Equations (4.4) and (4.5) together with the q -binomial recursion (see Stanley [26, Section 1.7]):

$$\begin{bmatrix} n \\ k \end{bmatrix}_q = \begin{bmatrix} n-1 \\ k \end{bmatrix}_q + q^{n-k} \begin{bmatrix} n-1 \\ k-1 \end{bmatrix}_q, \quad (4.6)$$

yield the desired formula:

$$\begin{aligned} \sum_{w \in \mathcal{L}(n, k)} q^{\widetilde{\text{maj}}(w)} &= \sum_{w \in \mathcal{L}_0(n, k)} q^{\widetilde{\text{maj}}(w)} + \sum_{w \in \mathcal{L}_1(n, k)} q^{\widetilde{\text{maj}}(w)} \\ &= q^k \begin{bmatrix} n+k-1 \\ k \end{bmatrix}_q + q^{n+k} \begin{bmatrix} n+k-1 \\ k-1 \end{bmatrix}_q \\ &= q^k \begin{bmatrix} n+k \\ k \end{bmatrix}_q. \end{aligned}$$

□

Lemma 4.12. There is a bijection between the sets $\mathcal{L}(n, k) \setminus \mathcal{Y}(n, k)$ and $\mathcal{L}(n+1, k-1)$ that reduces $\widetilde{\text{maj}}$ by one.

Proof. The same bijection used in the bijective proof of (4.1) by F\"urlinger and Hofbauer [11] applies here. Geometrically, we represent words in $\mathcal{L}(n, k)$ as lattice paths from $(0, 0)$ to (k, n) , where each letter 0 corresponds to an up step, and each 1 corresponds to a right step. The words in $\mathcal{L}(n, k) \setminus \mathcal{Y}(n, k)$ correspond to those lattice paths that must cross the diagonal.

Given such a path, consider the lattice point with the smallest x -coordinate that lies below the diagonal with maximal vertical distance from the diagonal. Call this point P . Let P' be the lattice point immediately preceding P along the path. By construction, the step from P' to P must be a right step. Replace this step with an up step, and denote the resulting point by P'' . We illustrate this bijection in Figure 42. □

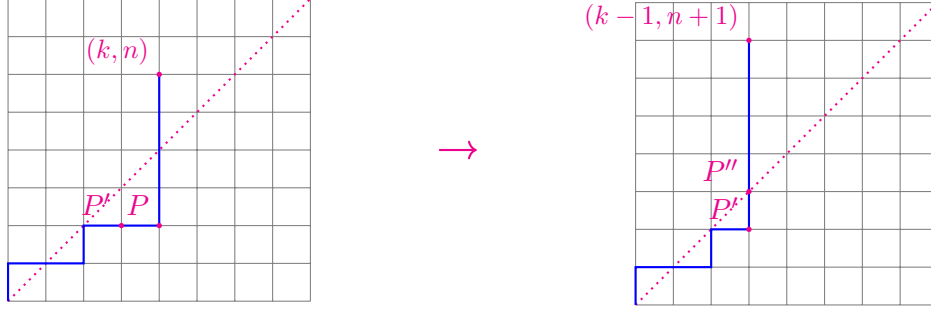


Figure 42: a bijection, due to Furlinger and Hofbauer

Proof of Proposition 4.10. Using Lemmas 4.11 and 4.12, we obtain

$$\begin{aligned}
\sum_{w \in \mathcal{Y}(n,k)} q^{\widetilde{\text{maj}}(w)} &= \sum_{w \in \mathcal{L}(n,k)} q^{\widetilde{\text{maj}}(w)} - \sum_{w \in \mathcal{L}(n,k) \setminus \mathcal{Y}(n,k)} q^{\widetilde{\text{maj}}(w)} \\
&= \sum_{w \in \mathcal{L}(n,k)} q^{\widetilde{\text{maj}}(w)} - q \cdot \sum_{w \in \mathcal{L}(n+1,k-1)} q^{\widetilde{\text{maj}}(w)} \\
&= q^k \begin{bmatrix} n+k \\ k \end{bmatrix}_q - q \cdot q^{k-1} \begin{bmatrix} n+k \\ k-1 \end{bmatrix}_q \\
&= q^{2k} \frac{[n-k+1]_q}{[n+1]_q} \begin{bmatrix} n+k \\ n \end{bmatrix}_q,
\end{aligned}$$

where the last equality is a basic computation with q -binomials. □

Proposition 4.10 will be used in Subsection 4.2. In Subsection 4.3, we make use of the following connecting statement.

Proposition 4.13. (i) Let $w \in \mathcal{Y}(n, k)$. Then $\text{comaj}(w) = \widetilde{\text{maj}}(w) - k$.

(ii) We have

$$\sum_{w \in \mathcal{Y}(n,k)} q^{\text{comaj}(w)} = q^k Y_q(n, k).$$

(iii) Let \bar{w} denote the reverse word of w , that is, $\bar{w} := w_\ell \dots w_1$ if $w = w_1 \dots w_\ell$. Then we have

$$\sum_{w \in \mathcal{Y}(n,k)} q^{\text{maj}(\bar{w})} = \sum_{w \in \mathcal{Y}(n,k)} q^{\text{comaj}(w)}.$$

Proof. The sum of the starting positions of the strings of 0's equals the sum of the starting positions of the strings of 1's minus the total number of 1's. This proves part (i).

Part (ii) follows directly from Proposition 4.10 and part (i) of this proposition.

Reversing a binary word of length n turns an ascent at position i into a descent at position $n - i$. By part (ii), the generating function of comaj on $\mathcal{Y}(n, k)$ is a palindromic polynomial. This completes part (iii). □

4.2 Decomposition formula for $\mathcal{P}_{1,b}$

In this subsection, we consider the restriction of the affine crystal graph $\mathcal{B}_{1,b}^{\mathcal{P}}$ to the blue arrows. Our strategy for obtaining a new infinite summation formula is as follows. We first describe the starting points of the blue strings. For each starting point, we determine the length of the corresponding blue string. The infinite summation formula is obtained by parametrising starting points according to their type. The summation formula coincides with the rank generating function of the affine crystal graph $\mathcal{B}_{1,b}^{\mathcal{P}}$, namely $(-q; q)_{\infty}$, and thus yields the desired identity. Moreover, the same procedure can be applied to the green arrows, leading to another summation formula.

We now focus on the blue arrows. A *starting point* in $\mathcal{B}_{1,b}^{\mathcal{P}}$ is a partition in $\mathcal{P}_{1,b}$ that is not the target of a blue arrow; equivalently, it is the initial vertex of a blue string in $\mathcal{B}_{1,b}^{\mathcal{P}}$. Recall from Definition 3.3 that λ is a starting point if and only if $\text{type}(\lambda)$ is a Yamanouchi word (we assign a left bracket “(” to 0, and a right bracket “)” to 1).

As long as the sequence of parts remains non-increasing, and we do not change the number of columns, adding or removing an even number of cells from a column does not change the type. In particular, there are infinitely many starting points with the same type.

Definition 4.14. For a Yamanouchi word w , we define the *pivot* to be the smallest partition λ with $\text{type}(\lambda) = w$, with respect to inclusion of diagrams.

Lemma 4.15. Pivots are in bijection with Yamanouchi words of even length.

Proof. If λ is a conjugate distinct-part partition with $2k - 1$ columns, then the first row of λ ends in a green cell. Thus, $\text{type}(\lambda) = r0$, where r is the binary word of length $2k - 1$ obtained by reading the bottom cells in the columns of λ from left to right. If λ has $2k$ columns, then the first row of λ ends in a blue cell. Thus, $\text{type}(\lambda) = r$, where r is the binary word of length $2k$ obtained by reading the bottom cells in the columns of λ from left to right. Therefore, $\text{type}(\lambda)$ has even length for any partition λ .

If $\text{type}(\lambda)$ has length $2k$, then λ has $2k - 1$ or $2k$ columns. Moreover $\text{type}(\lambda)$ determines the parity of each column. Among such partitions, there is a unique minimal element with respect to inclusion of diagrams.

This correspondence is illustrated in Figure 43. □

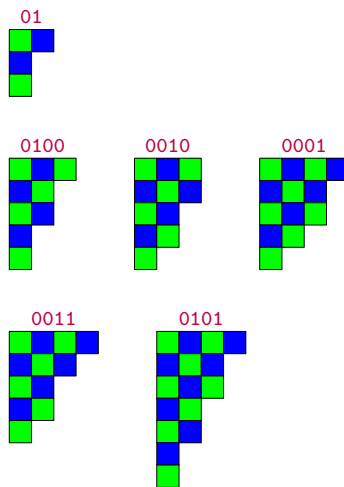


Figure 43: Correspondence between pivots and Yamanouchi words of even length

The following lemma shows that the size of a pivot can be expressed in terms of the binary word $\text{type}(\lambda)$.

Lemma 4.16. Let λ be a pivot with $w = \text{type}(\lambda) \in \mathcal{Y}(n, k)$, where $n + k$ is even and $n \geq k \geq 0$. Then we have

$$|\lambda| = \binom{n+k}{2} + 2\widetilde{\text{maj}}(w) - k.$$

Proof. We begin with a staircase shape of length $n + k - 1$, which is one less than the length of the word w . The pivot λ is then obtained from this staircase by adding suitable cells diagonally, which we explain in the next paragraph. We illustrate this construction in Figure 44. We denote by $\Psi(w)$ the partition whose parts correspond to the diagonals that are added.

The largest part of $\Psi(w)$, i.e. number of cells along the first (blue) diagonal, is the largest descent of the word $w0$, i.e. the word obtained from w by appending a letter 0 at the end. The second part of $\Phi(w)$, i.e. the number of cells along the second (green) diagonal, is the largest ascent of w . The third part of $\Phi(w)$ is the second largest descent, then the second largest ascent, and so on. Then λ is the partition obtained by adding these diagonals to the staircase.

For example, the Yamanouchi word $w = 00010011$ corresponds to the pivot illustrated in Figure 44. The associated partition of diagonals is $\Psi(w) = (8, 6, 4, 3)$.

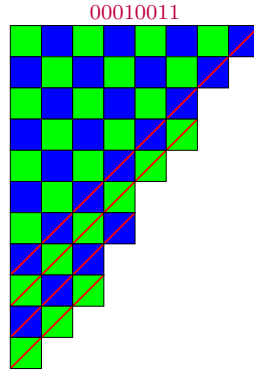


Figure 44: Another partition from a pivot

To see that any partition constructed in this way is a pivot, note that in the staircase consecutive parts differ by at most one, and we add at most one more cell to column i than to column $i + 1$ along the diagonals.

By definition, the contribution of the blue parts is $\widetilde{\text{maj}}(w)$ for each $w \in \mathcal{Y}(n, k)$ and the contribution of the green parts is $\text{comaj}(w)$. Therefore, by Proposition 4.13 (i), the size $|\Psi(w)|$ is given by $2\widetilde{\text{maj}}(w) - k$. \square

Let μ be a starting point with $\text{type}(\mu) = w \in \mathcal{Y}(n, k)$, where $n + k$ is even, and $n \geq k \geq 0$. Then there exists a unique pivot λ with the same type w , and μ can be obtained from λ in a unique way by adding even numbers $b_1 \geq \dots \geq b_{n+k}$ to the columns of its Young diagram, beginning with the first column. Therefore, we have the size generating function for starting points for a fixed pivot.

Lemma 4.17. The size generating function of starting points corresponding to a pivot λ with $\text{type}(\lambda) \in \mathcal{Y}(n, k)$ is

$$q^{|\lambda|} (q^2; q^2)_{n+k}^{-1}.$$

We are now ready to show the following identity, which relates the infinite product $(-q; q)_\infty$ to q -Yamanouchi numbers. This identity is also stated in Theorem 1.16.

Theorem 4.18. We have

$$(-q; q)_\infty = \sum_{n \geq k \geq 0} q^{n(2n-1)+3k} Y_{q^2}(2n-k, k) (q^2; q^2)_{2n}^{-1} [2(n-k)+1]_q.$$

Proof. Let λ be a pivot with $w = \text{type}(\lambda) \in \mathcal{Y}(n, k)$, where $n+k$ is even and $n \geq k \geq 0$. By Lemma 4.16 and Lemma 4.17, the generating function of starting points whose pivot is λ is

$$q^{\binom{n+k}{2} + 2\widetilde{\text{maj}}(w) - k} (q^2; q^2)_{n+k}^{-1}.$$

All strings whose starting point has pivot λ have length $n-k$, which is the number of unmatched 0s in $\text{type}(\lambda)$. Each arrow increases the size by one. Hence we multiply the generating function by $[n-k+1]_q$.

To simplify the condition for n and k , replace n by $2n-k$. The infinite summation formula, obtained by summing the product of the size generating function of starting points and the length of its blue string, is equal to

$$\sum_{n \geq k \geq 0} \sum_{w \in \mathcal{Y}(2n-k, k)} q^{\binom{2n}{2} + 2\widetilde{\text{maj}}(w) - k} (q^2; q^2)_{2n}^{-1} [2(n-k)+1]_q.$$

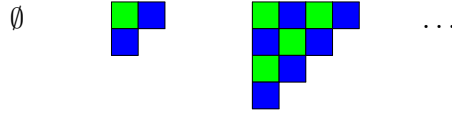
By Proposition 4.10, we obtain the desired result. □

We could also consider the restriction formula obtained by erasing the blue arrows in the affine crystal graph $\mathcal{B}_{1,b}^P$ (see Figure 1), instead of the green arrows. We obtain the second formula in Theorem 1.16.

Theorem 4.19. We have

$$(-q; q)_\infty = \sum_{n \geq k \geq 0} q^{(2n+1)n+3k} Y_{q^2}(2n+1-k, k) (q^2; q^2)_{2n+1}^{-1} [2(n-k)+2]_q.$$

Proof. The same argument goes through as in the proof of Theorem 1.16, with the only difference that we start building from an even staircase,



and the length of each green string is odd. □

Remark 4.20. Note that this is equivalent to restricting the affine crystal graph of highest weight Λ_1 and type $A_1^{(1)}$ to blue arrows. The partition model for this graph is the same as Definition 3.3, but each partition has a blue cell in the top-left corner instead of a green cell.

4.3 Decomposition formula for $\mathcal{P}_{2,b}$

In this subsection, we consider the restriction of the affine crystal graph $\mathcal{B}_{2,b}^P$ to the blue arrows. Once again, the connected infinite crystal graph $\mathcal{B}_{2,b}^P$, illustrated in Figure 2, breaks into a disjoint union of infinitely many blue strings of finite length. Based on this decomposition, we express the infinite product $(-q; q^2)_\infty / (q; q^2)_\infty$ as an infinite sum of q -binomial expressions.

In Subsection 4.2, we described starting points in terms of the type. Then, we computed the generating function for pivots, the smallest partitions with given type. Similarly, in the graph $\mathcal{B}_{2,b}^{\mathcal{P}}$, a vertex π is a starting point if and only if $\text{type}(\pi)$ is a Yamanouchi word.

Here, it is convenient to provide an alternative description that uses the colour sequence of the parts of π instead of the type. In this approach, we define the pivot in a different way, again as the smallest partition in an appropriate sense, and derive the decomposition formula. Note that the type of π is obtained from the bottommost cells in each column of its Young diagram, whereas considering the colour sequence of the parts is obtained from the rightmost cells in each row.

Definition 4.21. A *starting point* in $\mathcal{B}_{2,b}^{\mathcal{P}}$ is a grounded partition in $\mathcal{P}_{2,b}$ that is not the target of a blue arrow. A starting point in $\mathcal{B}_{2,b}^{\mathcal{P}}$ is called a *pivot* if it has no b -parts. We denote by $\text{PIV}(n, k)$ the set of pivots with n many a -parts and k many c -parts.

Lemma 4.22. Let $\pi \in \mathcal{P}_{2,b}$ be a grounded partition with n many a -parts, k many c -parts and no b -parts. Then

- (i) π is a starting point if and only if its sequence of colours, read from the smallest nonzero part upward, forms a Yamanouchi word, where a is interpreted as 0, and c as 1.
- (ii) If π is a starting point with corresponding Yamanouchi word $w \in \mathcal{Y}(n, k)$, then the length (i.e. the number of blue arrows) of the blue string starting from π is $2(n - k) + 1$.

Proof. For a starting point π , the word $\text{type}(\pi)$ starts with 0. Hence, the first part of π is 1_a . An a -part that follows an a -part contributes 00 to $\text{type}(\pi)$. An a -part that follows a c -part lies in the same column, and therefore it does not contribute to $\text{type}(\pi)$. Similarly, a c -part that follows an a -part does not contribute to $\text{type}(\pi)$. A c -part that follows a c -part contributes 11 to $\text{type}(\pi)$.

Let w be the binary word obtained from the colour sequence of the parts of π . The above argument shows that $\text{type}(\pi)$ is a Yamanouchi word if and only if w is a Yamanouchi word. This proves the first statement.

Moreover, after the first letter 0, we have $2(n - k)$ many unmatched 0s, so the length of the blue string starting from π is $2(n - k) + 1$. \square

Next, we consider arbitrary starting points, not only pivots.

Lemma 4.23. A grounded partition $\pi \in \mathcal{P}_{2,b}$ is a starting point if and only if the subsequence of colours, starting from the smallest nonzero part and restricted to the letters a and c , forms a Yamanouchi word, with a interpreted as 0 and c as 1. Moreover, the number of b -parts does not affect the length of the corresponding blue string.

Proof. A *string of b -parts* in π is a maximal sequence of consecutive b -parts $k_b k_b \dots k_b$, that is, all the b -parts of the same size. We proceed by induction on the number of strings of b -parts. The base case is Lemma 4.22, where π has no b -parts. Assume the statement holds for all π with at most i strings of b -parts. Let $k_b k_b \dots k_b$ denote the $(i + 1)$ th string. Let $\tilde{\pi} \in \mathcal{P}_{2,b}$ be the grounded partition that has the same colour sequence as π , except that the $(i + 1)$ th string of b 's is removed from the colour sequence (note that there is a unique grounded partition in $\mathcal{P}_{2,b}$ with a given colour sequence). For example, for $\pi = 1_a 1_c 1_a 2_b 2_b 3_a$ we have $\tilde{\pi} = 1_a 1_c 1_a 3_a$; for $\pi = 1_a 1_c 2_b 3_a$ we have $\tilde{\pi} = 1_a 1_c 1_a$.

First, assume that π also contains a part of size $k + 1$, i.e. k_b is not the largest part. We then distinguish four cases, according to the colours of the odd parts that precede and follow the $(i + 1)$ th string of b -parts.

- (1a) Assume the $(i + 1)$ th string of b -parts in π lies between two a -parts, $(k - 1)_a$ and $(k + 1)_a$. This is illustrated in Figure 45. Since the difference between two consecutive a -parts is 2, the number of columns in π and $\tilde{\pi}$ is

the same. Because a and c alternate in the odd columns and the part preceding the first b -part is an a -part, the bottom cell in the k th column is a green b -cell in both cases. Therefore, $\text{type}(\pi) = \text{type}(\tilde{\pi})$. Hence π is a starting point if and only if $\tilde{\pi}$ is a starting point, and in this case, the length of the corresponding strings is the same.

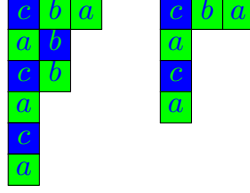


Figure 45: String of bs between two a -parts

- (1b) Assume the $(i + 1)$ th string of b -parts is preceded by an a -part $(k - 1)_a$ and followed by a c -part $(k + 1)_c$. This case is illustrated in Figure 46.

In π , the column of bs has a green cell at the bottom and the next column has a c -cell at the bottom, which contributes the factor 01 to $\text{type}(\pi)$. In $\tilde{\pi}$, these two columns disappear and all other column endings are unchanged. Therefore, $\text{type}(\pi) \sim \text{type}(\tilde{\pi})$.

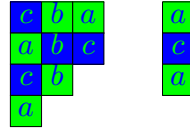


Figure 46: String of bs between an a -part and a c -part

- (1c) Assume the $(i + 1)$ th string of b -parts is preceded by a c -part $(k - 1)_c$ and followed by an a -part $(k + 1)_a$. This case is illustrated in Figure 47. In π , we have three consecutive columns ending in a , b and a , where the b -cell is blue. This contributes the factor 010 to $\text{type}(\pi)$. In $\tilde{\pi}$, two of these columns disappear, which yields the factor 0 . Therefore, $\text{type}(\pi) \sim \text{type}(\tilde{\pi})$.

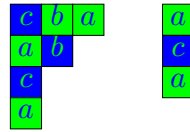


Figure 47: String of bs between a c -part and an a -part

- (1d) Assume the $(i + 1)$ th string of b -parts lies between two c -parts k_c and $(k + 2)_c$. Since the difference between two consecutive c -parts is 2 , the number of columns in π and $\tilde{\pi}$ is the same. Because a and c alternate in the odd columns, the bottom b -cell is blue in both cases. This is illustrated in Figure 48. Therefore, $\text{type}(\pi) = \text{type}(\tilde{\pi})$.

Finally, assume that π ends with the $(i + 1)$ th string of bs . We distinguish two cases, according to the colour of the preceding odd part.

- (2a) Assume the last string of bs follows an a -part k_a . Then the last column of bs in π has a green cell at the bottom, which contributes a letter 0 to $\text{type}(\pi)$. Since the largest part of π is $(k + 1)_b$, the first row of π ends

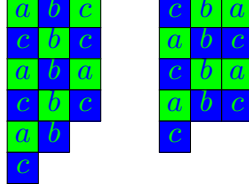


Figure 48: String of b s between two c -parts

in a b -cell, which contributes another letter 0 at the end of $\text{type}(\pi)$. In $\tilde{\pi}$, the largest part is k_a , so the first row of $\tilde{\pi}$ ends in an a -cell, which contributes 00 at the end of $\text{type}(\tilde{\pi})$. Therefore, $\text{type}(\pi) = \text{type}(\tilde{\pi})$. This case is illustrated in Figure 49.

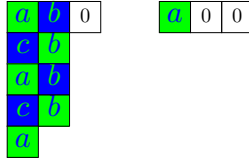


Figure 49: Largest part is a b , preceded by an a -part

- (2b) Assume the last string of b 's follows a c -part k_c , and that $(k+1)_b$ is the largest part in π . This case is illustrated in Figure 50. Then the last column of b 's has a blue cell at the bottom, and the first row of π contributes to $\text{type}(\tilde{\pi})$ with an extra letter 0. Therefore, $\text{type}(\tilde{\pi})$ is obtained from $\text{type}(\pi)$ by removing the right factor 10.

First, assume that π is a starting point. By Lemma 4.22 (ii), the blue string starting from π has odd length. In particular, by the induction hypothesis, there is at least one unmatched letter 0 in $\text{type}(\tilde{\pi})$. Therefore, the letter 1 in the right factor 10 of $\text{type}(\pi)$ gets matched. The letter 0 in the right factor 10 is unmatched. Hence, $\text{type}(\pi) \sim \text{type}(\tilde{\pi})$.

Next, assume π is not a starting point, i.e. $\text{type}(\tilde{\pi})$ is not a Yamanouchi word. In this case, $\text{type}(\pi)$ and $\text{type}(\tilde{\pi})$ are not necessarily equivalent. However, after erasing the right factor 10 from $\text{type}(\pi)$, the word $\text{type}(\tilde{\pi})$ remains non-Yamanouchi, i.e. $\tilde{\pi}$ is also not a starting point.

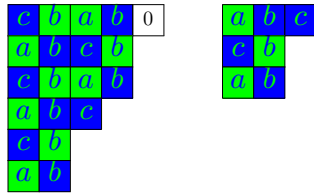


Figure 50: Largest part is a b , preceded by a c -part

□

We need to compute the size generating function of pivots in $\text{PIV}(n, k)$.

Example 4.24. Consider the pivots with four a -parts and two c -parts:

$$1_a 3_a 5_a 7_a 7_c 9_c, 1_a 3_a 5_a 5_c 5_a 5_c, 1_a 3_a 3_c 3_a 5_a 5_c, 1_a 1_c 1_a 3_a 5_a 5_c, 1_a 3_a 5_a 5_c 7_c 7_a,$$

$$1_a 3_a 3_c 3_a 3_c 3_a, 1_a 1_c 1_a 3_a 3_c 3_a, 1_a 3_a 3_c 5_c 5_a 7_a, 1_a 1_c 1_a 1_c 1_a 3_a.$$

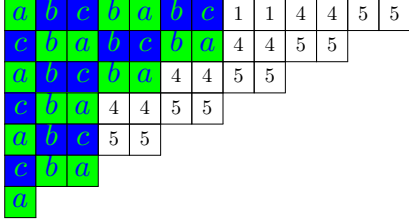


Figure 51: Obtaining $\pi = 1_a 3_a 3_c 3_a 5_a 7_a 7_c$ from the odd staircase

Their size generating function is given by

$$q^8 + q^{12} + 2q^{16} + q^{20} + 2q^{24} + q^{28} + q^{32} = q^8 Y_{q^4}(4, 2).$$

Lemma 4.25. Let $\pi \in \text{PIV}(n, k)$ be a pivot whose parts are coloured only a or c . Let $w \in \mathcal{Y}(n, k)$ denote the word obtained by replacing a by 0 and c by 1 in the colour sequence of π . Then we have

$$|\pi| = (n + k)^2 - 4 \widetilde{\text{maj}}(\bar{w}) + 2k,$$

where \bar{w} denotes the reverse word of w .

Proof. We begin with an odd staircase of length $n + k$. The size of this staircase is $(n + k)^2$. Each descent i in \bar{w} that contributes to the modified major index decreases the size of the odd staircase by $2i$, since, instead of jumping by two, we have two repeated odd parts. Similarly, each ascent i —that is, a position where a 0 is followed by a 1—also decreases the size by $2i$. The proof is completed by Proposition 4.13 (i). \square

Example 4.26. Figure 51 illustrates the example $\pi = 1_a 3_a 3_c 3_a 5_a 7_a 7_c$ inside the odd staircase with 7 parts. In this example, the colour sequence is $aacaaac$, so the associated binary word is $w = 0010001$. The reverse word is $\bar{w} = 1000100$, which has descents at positions 1 and 5 and an ascent at position 4. In Figure 51, we first remove 5 pairs of cells from the top 5 rows of the odd staircase because of the descent at position 5, then remove 4 pairs of cells from the top 4 rows because of the ascent at position 4, and finally remove one pair of cells from the top row because of the descent at position 1.

Lemma 4.27. The size generating function of starting points corresponding to a pivot $\pi \in \text{PIV}(n, k)$ with n many a s and k many c s is given by

$$q^{|\pi|} (q^2; q^2)_{n+k}^{-1}.$$

Proof. Recall that the map defined in the proof of Theorem 2.3 gives a size-preserving bijection between

- (i) pairs (s, λ_e) where s is a sequence of colours a and c of length ℓ and λ_e is a partition into even parts, where the largest part is at most 2ℓ ,
- (ii) grounded partitions $\lambda \in \mathcal{P}_{2,b}$.

Moreover, the subsequence of colours restricted to the letters a and c in λ is s .

Fix s to be the colour sequence of the pivot π . This yields a size-preserving bijection between partitions into even parts, where the largest part is at most $2(n + k)$, and grounded partitions μ , whose colour subsequence consisting only of letters a and c is s . The size generating function for partitions into at most $n + k$ even factors is $(q^2; q^2)_{n+k}^{-1}$. \square

Now we are ready to prove the identity stated in Theorem 1.17.

Theorem 4.28. We have

$$\frac{(-q; q^2)_\infty}{(q; q^2)_\infty} = \sum_{n \geq k \geq 0} q^{2k+(n-k)^2} Y_{q^4}(n, k) (q^2; q^2)_{n+k}^{-1} [2(n-k) + 2]_q.$$

Proof. Using Lemma 4.25 and Proposition 4.13 (iii), the size generating function of pivots in $\text{PIV}(n, k)$ can be written as

$$\begin{aligned} \sum_{\pi \in \text{PIV}(n, k)} q^{\text{wt}(\pi)} &= q^{(n+k)^2} \cdot q^{-4k} Y_{-q^4}(n, k) \cdot q^{2k} \\ &= q^{(n+k)^2 - 2k} Y_{-q^4}(n, k). \end{aligned}$$

The minimal possible size in $\text{PIV}(n, k)$ is $2k+(n-k)^2$, realised by the grounded partition $1_a 1_c 1_a 1_c \dots 1_a 3_a 5_a \dots (2(n-k)-1)_a$ when $n > k$ and by $1_a 1_c \dots 1_a 1_c$ when $n = k$. Moreover, $Y_{q^4}(n, k)$ is a palindromic polynomial with constant term 1. Therefore, we obtain

$$\sum_{\pi \in \text{PIV}(n, k)} q^{\text{wt}(\pi)} = q^{2k+(n-k)^2} Y_{q^4}(n, k). \quad (4.7)$$

By Lemma 4.27, we multiply (4.7) by the factor $(q^2; q^2)_{n+k}^{-1}$, to get the generating function of all starting points. Finally, by Lemmas 4.22 and 4.23, if the pivot of a starting point lies in $\text{PIV}(n, k)$, then the length of the corresponding blue string is $2(n-k) + 1$. Hence we multiply the generating function by $[2(n-k) + 2]_q$, to obtain the identity. \square

Remark 4.29. In the affine crystal graph $\mathcal{B}_{2,b}^P$, erasing the blue arrows instead of the green arrows yields the same restriction formula, unlike in the case of $\mathcal{B}_{1,b}^P$, discussed in Subsection 4.2. This is clear from a representation-theoretic point of view: the affine crystal graph $\mathcal{B}_{2,b}^P \cong \mathcal{B}_{2,b}^A$ has highest weight $\Lambda_0 + \Lambda_1$, which is preserved by the involution induced by swapping Λ_0 and Λ_1 .

References

- [1] S. Ariki, V. Kreiman, and S. Tsuchioka. “On the tensor product of two basic representations of $U_v(\widehat{\mathfrak{sl}}_e)$ ”. In: *Advances in Mathematics* 218.1 (2008), pp. 28–86. DOI: 10.1016/j.aim.2007.11.018.
- [2] M. Bóna, ed. *Handbook of Enumerative Combinatorics*. Discrete Mathematics and Its Applications. Chapman & Hall / CRC Press, 2015, p. 1086. ISBN: 9780429170317.
- [3] D. Bump and A. Schilling. *Crystal Bases: Representations and Combinatorics*. World Scientific Publishing Company, 2017. ISBN: 9814733466.
- [4] L. Carlitz and J. Riordan. “Two-Element Lattice Permutation Numbers and Their q -Generalization”. In: *Duke Mathematical Journal* 31.3 (1964), pp. 371–388. DOI: 10.1215/S0012-7094-64-03136-9.
- [5] S. Chern, Z. Li, D. Stanton, T. Xue, and A. J. Yee. “The Ariki–Koike algebras and Rogers–Ramanujan type partitions”. In: *Journal of Algebraic Combinatorics* 60 (2024), pp. 491–540. DOI: 10.1007/s10801-024-01340-z.
- [6] S. Corteel and J. Lovejoy. “Overpartitions”. In: *Trans. Amer. Math. Soc.* 356.4 (2004), pp. 1623–1635. ISSN: 0002-9947, 1088-6850. DOI: 10.1090/S0002-9947-03-03328-2.

- [7] J. Dousse, L. Hardiman, and I. Konan. “Partition identities from higher level crystals of $A_1^{(1)}$ ”. In: *Proceedings of the American Mathematical Society* 153.4 (Feb. 2025), pp. 1363–1382. DOI: [10.1090/proc/16417](https://doi.org/10.1090/proc/16417). URL: <https://hal.science/hal-03448464>.
- [8] J. Dousse and I. Konan. *Generalisations of Capparelli’s and Primc’s identities, II: perfect $A_{n-1}^{(1)}$ crystals and explicit character formulas*. 2020. arXiv: 1911.13189 [math.QA]. URL: <https://arxiv.org/abs/1911.13189>.
- [9] J. Dousse and I. Konan. “Multi-grounded partitions and character formulas”. In: *Advances in Mathematics* 400 (2022), p. 108275. ISSN: 0001-8708. DOI: <https://doi.org/10.1016/j.aim.2022.108275>. URL: <https://www.sciencedirect.com/science/article/pii/S0001870822000913>.
- [10] O. Foda, B. Leclerc, M. Okado, J.-Y. Thibon, and T. Welsh. “Branching Functions of $A_{n-1}^{(1)}$ and Jantzen–Seitz Problem for Ariki–Koike Algebras”. In: *Advances in Mathematics* 141 (1997), pp. 322–365. URL: <https://api.semanticscholar.org/CorpusID:15556417>.
- [11] J. Fürlinger and J. Hofbauer. “q-Catalan numbers”. In: *Journal of Combinatorial Theory, Series A* 40.2 (1985), pp. 248–264. ISSN: 0097-3165. DOI: [https://doi.org/10.1016/0097-3165\(85\)90089-5](https://doi.org/10.1016/0097-3165(85)90089-5). URL: <https://www.sciencedirect.com/science/article/pii/0097316585900895>.
- [12] G. Gasper and M. Rahman. *Basic hypergeometric series*. Second. Vol. 96. Encyclopedia of Mathematics and its Applications. With a foreword by Richard Askey. Cambridge University Press, Cambridge, 2004, pp. xxvi+428. ISBN: 0-521-83357-4. DOI: [10.1017/CB09780511526251](https://doi.org/10.1017/CB09780511526251). URL: <https://doi.org/10.1017/CB09780511526251>.
- [13] M. Geck and N. Jacon. *Representations of Hecke Algebras at Roots of Unity*. Second. Vol. 15. Algebra and Applications. With a foreword by Richard Askey. Springer-Verlag, 2011.
- [14] J. Hong and S.-J. Kang. *Introduction to Quantum Groups and Crystal Bases*. Vol. 42. Graduate Studies in Mathematics. Amer. Math. Soc., 2002.
- [15] V. Kac. *Infinite Dimensional Lie Algebras*. 3rd. Cambridge Univ. Press, 1990.
- [16] S. Kang, M. Kashiwara, K. Misra, T. Miwa, T. Nakashima, and A. Nakayashiki. “Perfect crystals of quantum affine Lie algebras”. In: *Duke Mathematical Journal* 68.3 (1992), pp. 499–607. DOI: [10.1215/S0012-7094-92-06821-9](https://doi.org/10.1215/S0012-7094-92-06821-9).
- [17] C. Krattenthaler. “Counting lattice paths with a linear boundary I”. In: *Sitz.ber. d. ÖAW Math.-naturwiss. Klasse* 198 (1989), pp. 87–107.
- [18] C. Krattenthaler. “Counting lattice paths with a linear boundary II”. In: *Sitz.ber. d. ÖAW Math.-naturwiss. Klasse* 198 (1989), pp. 171–199.
- [19] J. Lepowsky and S. Milne. “Lie Algebraic Approaches to Classical Partition Identities”. In: *Advances in Mathematics* 29.1 (1978), pp. 15–59. ISSN: 0001-8708. DOI: [https://doi.org/10.1016/0001-8708\(78\)90004-X](https://doi.org/10.1016/0001-8708(78)90004-X). URL: <https://www.sciencedirect.com/science/article/pii/000187087890004X>.
- [20] J. Lepowsky and R. L. Wilson. “The structure of standard modules, I: Universal algebras and the Rogers-Ramanujan identities”. In: *Invent. Math.* 77 (1984), pp. 199–290. DOI: <https://doi.org/10.1007/BF01388447>.
- [21] J. Lepowsky and R. L. Wilson. “The structure of standard modules, II: The case $A_1^{(1)}$, principal gradation”. In: *Invent. Math.* 79 (1985), pp. 417–442. DOI: <https://doi.org/10.1007/BF01388515>.
- [22] P. A. MacMahon. *Combinatory Analysis*. Vol. 2. New York, NY, USA: Cambridge Univ. Press, 1916.
- [23] L. J. Rogers and S. Ramanujan. “Proof of certain identities in combinatory analysis”. In: *Math. Proc. Cambridge Philos. Soc.* 19 (1919), pp. 211–216.

- [24] I. Schur. “Ein Beitrag zur Additiven Zahlentheorie und zur Theorie der Kettenbrüche”. In: *S.-B. Preuss. Akad. Wiss. Phys. Math. Klasse* (1917), pp. 302–321.
- [25] A. V. Sills. *An invitation to the Rogers-Ramanujan identities*. With a foreword by G. E. Andrews. CRC Press, Boca Raton, FL, 2018, pp. xx+233. ISBN: 978-1-4987-4525-3.
- [26] R. P. Stanley. *Enumerative Combinatorics, Volume 2*. Vol. 62. Cambridge Studies in Advanced Mathematics. Cambridge, UK: Cambridge University Press, 1999. ISBN: 0-521-56069-1. DOI: 10.1017/CB09780511609589.
- [27] M. Wakimoto. *Lectures on Infinite-dimensional Lie Algebra*. Singapore: World Scientific Publishing Co. Pte. Ltd., 2001. ISBN: 9814494003; 9789814494007.